Effect of Zinc Availability on the Morphology and Nutrient Physiology of a Coastal and an Oceanic Diatom

by

Valeria Willers
Licenciatura Cs. Bs., Universidad Nacional de la Patagonia, 2004

A Thesis Submitted in Partial Fulfillment
of the Requirements for the Degree of

MASTER OF SCIENCE

in the Department of Biology

SUPERVISORY COMMITTEE

Effect of Zinc Availability on the Morphology and Nutrient Physiology of a Coastal and an Oceanic Diatom

by

Valeria Willers

B.Sc., Universidad Nacional de la Patagonia, 2004

Supervisory Committee

Dr. Diana E. Varela, Supervisor
(Department of Biology & School of Earth and Ocean Sciences)

Dr. Jay T. Cullen
(School of Earth and Ocean Sciences)

Dr. Real Roy
(Department of Biology)

Supervisory Committee

Dr. Diana E. Varela, Supervisor
(Department of Biology & School of Earth and Ocean Sciences)

Dr. Jay T. Cullen
(School of Earth and Ocean Sciences)

Dr. Real Roy
(Department of Biology)

ABSTRACT

Low dissolved zinc concentrations in marine waters can limit growth and productivity of phytoplankton, as Zn is a required component of critical enzymes such as carbonic anhydrase. This thesis examined the effects of Zn availability on growth rates, cell morphology, elemental composition and ratios, and incorporation rates of macronutrients in the coastal diatom *Skeletonema costatum* and the oceanic diatom *Thalassiosira oceanica*. Under Zn limitation, *S. costatum* exhibited a decrease in maximum growth rate (60%), chlorophyll content (20%) and an increase in the surface to volume (S/V) ratio (80%) compared to Zn-replete cells. In *S. costatum* elemental quotas showed a decrease in silicon content (20%) and a significant increase in carbon content (52%) and phosphorus content (55%). Moreover, silicon content per surface area significantly decreased by 50% under Zn limitation. Elemental ratios showed significant differences only for Si:C and Si:N between Zn-replete and Zn limiting conditions. The elemental stoichiometry of *S. costatum* was 82C : 9N : 5Si : 1P under Zn-limiting

conditions compare to 84C : 12N : 9Si : 1 P under Zn-replenishment. In *T. oceanica*, Zn limitation was also responsible for a decrease in maximum growth rate (60%) and chlorophyll content (20%) compared to Zn-replete cells, but Zn limitation did not affect the S/V ratio. Elemental quotas and ratios in *T. oceanica* did not exhibit significant differences under Zn limitation. However, nitrogen, silicon and phosphorus content showed a 20% increasing trend in Zn-limited cells. Elemental quotas for *T. oceanica* were 51C : 6N : 2Si : 1P under Zn-limitation and 71C : 6N : 2Si : 1P under Zn-replenishment. These laboratory experiments suggest that Zn availability in the oceans can affect the stoichiometry of nutrient uptake and the structure of phytoplankton assemblages, especially in coastal environments.

TABLE OF CONTENTS

LIST OF TABLES

LIST OF FIGURES

LIST OF ABBREVIATIONS

BSi	Biogenic silica
C	Carbon
CA	Carbonic anhydrase
Cd	Cadmium
Chl-*a*	Chlorophyll *a*
Co	Cobalt
DNA	Deoxyribonucleic acid
EDTA	Ethylenediaminetetraacetic acid
Fe	Iron
HNLC	High nitrate, low chlorophyll
$K_{S\text{-}Zn}$	Half saturation constant for growth
M	Molar
N	Nitrogen
NO_3^-	Nitrate
OSP	Ocean Station Papa
P	Phosphorus
PC	Polycarbonate
Pg	Petagram ($= 10^{15}$)
POC	Particulate organic carbon
PON	Particulate organic nitrogen
POP	Particulate organic phosphorus
HPO_4^{2-}	Phosphate
S	Cell surface area
SEM	Scanning electron microscope
Si	Silicon
$Si(OH)_4$	Silicic acid
TMC	Trace metal clean
V	Cell volume
Zn	Zinc
μ	Specific growth rate
μ_{max}	Maximum specific growth rate

ACKNOWLEDGMENTS

I would like to thank Dr. Diana Varela for her guidance and support during my master thesis. I appreciate a lot the freedom you gave me to chose and pursue a project I was interested in. I would like also to thanks my committee members, Dr. Jay Cullen and Dr. Real Roy, who were always available for questions. Your advice and thoughts in committee meeting and informal meetings were always very helpful.

Special thanks to Dr. Maite Maldonado for the generous and great opportunity to learn trace metal clean techniques and phytoplankton culture in her lab. Thanks to Keith Jonhson for collecting seawater from St.P, which made possible all my culture work.

Thanks to my lab mates Brianne Kelly, Damian Grundle, Ian Wrohan and Samantha Robbins that were always happy to help. Also thanks to Vasko, Nicole and David for their help with proofreading and the microscope!

I gratefully thanks the funding received from University of Victoria Fellowship, Organization of American States Fellowship and Randy Baker Memorial Scholarship.

To Laura, Diego, Carmen, Antonio, Caroll, Holly, Irena, Jany and Julio, thank you! Among 'tardes con mates', camping, brewing, kayaking, hard times and laugh, I was happy to share your friendship and get to know each of you.

To my parents, that gave me the encouragement, support and confidence to pursue my projects.

CHAPTER 1 – INTRODUCTION

1.1. GENERAL INTRODUCTION

Diatoms belong to a large phytoplankton group (Bacillariophyceae) that plays an important role in oceanic biological productivity. Diatoms can account for up to 40% of the total marine primary production, which has been estimated at 50 Pg of carbon per year (Nelson et al., 1995; Falkowski et al., 1998). Their contribution to primary production can range from 35% in oligotrophic oceans to 75% in coastal areas and the Antarctic (Treguer et al., 1995). In addition, diatoms are responsible for 20% to 90% of the total organic carbon exported to the deep sea, estimated at 12±4 Pg per year (Sarmiento and Gruber, 2006). Therefore, understanding the physiology and nutrient requirements of diatoms is fundamental for determining the mechanisms that control their production, and for evaluating their role in the biological carbon pump and drawdown of atmospheric CO_2.

Models of biogeochemical cycles usually employ a Redfield ratio of 106 Carbon(C) : 16 Nitrogen(N) : 1 Phosphorus (P) (Redfield, 1958) to describe the elemental composition of phytoplankton, and to link primary production with the cycles of carbon to nitrogen and phosphorus. In the case of diatoms, silicon (Si) is added to this equation with a mean Si:N value of 1.05 (~1) (Brzezinski, 1985). However, recent studies have shown that variations in the concentration of micronutrients such as iron (Fe) and zinc (Zn) can affect the ratios at which macronutrients are incorporated into the cells (Hutchins and Bruland, 1998; De La Rocha et al., 2000; Franck et al., 2003). Thus, further research is needed to better understand the effects that the physiological responses

of diatoms to environmental stress factors have on macronutrient uptake and elemental composition.

Low concentrations of Zn in the marine environment can limit the growth and productivity of phytoplankton as well as affect the distribution of phytoplankton species and their dominance in the oceans (Brand et al, 1983; Crawford et al., 2003; Leblanc et al., 2005). Zn is an important micronutrient because it is the component of many essential enzymes such as carbonic anhydrase (CA). Since CA has a critical role in the carbon acquisition mechanism, Zn availability can affect macronutrient uptake ratios in phytoplankton. In addition, a few studies have also shown that Zn can affect $Si(OH)_4$ and NO_3^- uptake kinetics (De la Rocha et al., 2000; Franck et al., 2003). As a result, Zn availability in the marine environment may be partly responsible for changes in the Si/C and Si/N ratios.

The aim of the present study was to further understand the role of Zn in the morphology and nutrient physiology of diatoms. More specifically, this project addressed the effect of Zn limitation on maximum growth rates, cell size, macronutrient uptake, and the elemental composition and stoichiometry of C, N, Si and P in a coastal and an oceanic diatom. Extrapolation of the results from these laboratory experiments to a field scenario should provide a better understanding of the effects of Zn availability on natural phytoplankton assemblages.

1.2. ELEMENTAL RATIOS OF CARBON, NITROGEN, PHOSPHORUS AND SILICON IN MARINE PHYTOPLANKTON

In 1934, Redfield proposed that C, N and P are present in seawater and in plankton (i.e., phytoplankton and zooplankton) in constant ratios. On average, for each atom of P in phytoplankton there are 16 atoms of N and 106 atoms of C, and this C:N:P ratio of 106:16:1 is known as the Redfield ratio (Redfield, 1958). Through the processes of nutrient uptake and incorporation, and export of organic matter to the deep ocean, phytoplankton play a significant role in the cycling and distribution of these major nutrients. In this way, the distribution of C, N and P (as well as those of other nutrients) in the oceans are linked to phytoplankton primary productivity.

In addition to C, N and P, diatoms have a unique requirement for Si. The cell wall (frustule) is composed of hydrated amorphous silica ($SiO_2.nH_2O$) (Martin-Jezequel et al., 2000). In the oceans, diatoms are the main organisms that take up dissolved Si (as silicic acid, $Si(OH)_4$) and thus they dominate the biogeochemical cycling of Si in the sea (Treguer et al., 1995; Sarmiento and Gruber, 2006). Brzezinski (1985) studied the nutrient stoichiometry in diatoms and found that the average values of Si:C and Si:N ratio in 27 diatoms species were 0.13 and 1.05, respectively.

A thorough understanding of the factors that control the ratios at which nutrients are found in phytoplankton requires further research. Recent studies explained the elemental stoichiometry of phytoplankton in terms of the role of C, N and P in the constitution of major macromolecules along with the relative proportions of these nutrients required for the cell's growth and resources acquisition (Geider and La Roche,

2002; Klausmeier et al., 2004). This link between cell functioning and elemental composition was used to model and explain the optimal nitrogen N to P stoichiometry in phytoplankton (Klausmeier et al., 2004). The model predicted that under scarce resources (competitive equilibrium), slow-growing phytoplankton favor greater allocation to N-rich resource-acquisition machinery, which results in a N:P ratio of >30. In contrast, bloom forming phytoplankton increase the production of growth machinery (P-rich), reducing their N:P ratio to ~8. Thus, the Redfield N:P ratio of 16:1 seems to represent an average for phytoplankton assemblages that use different growth strategies under different environmental conditions.

The elemental composition of phytoplankton can also vary considerably among species and with environmental stress factors. Ho et al. (2003) showed that there is interspecific variability in the C:N:P stoichiometry in cultured phytoplankton. Furthermore, variations in elemental ratios can result from changes in the composition of macromolecules and internal nutrient pools due to physiological responses to nutrient limitation and light regimes (Geider and La Roche, 2002). Under nutrient limitation, cell growth rate decreases and thus the duration of the cell cycle is extended. Consequently, an increase in the duration of a particular stage in the cell cycle can result in a higher requirement for a given nutrient (Claquin et al., 2002). For example, the amount of Si incorporated by diatoms is mainly linked to the duration of the phase corresponding to cell wall synthesis (Martin-Jezequel et al., 2000). An increase in the length of this stage under low growth conditions allows maximum incorporation of Si onto the frustule (Martin-Jezequel et al., 2000). Moreover, an uncoupling of Si incorporation from the C and N metabolisms has been reported for *Thalassiosira pseudonana* under light, nitrogen

and phosphorus limitation (Claquin et al., 2002). Therefore, the relationship between cell metabolism and growth rate can have important effects on the elemental composition and stoichiometry of a phytoplankton cell.

Micronutrient limitation has also been shown to affect the elemental composition of marine phytoplankton, however, most studies focused on Fe. Iron was shown to have an influence on $Si(OH)_4$ and NO_3^- uptake rates in natural phytoplankton assemblages (Hutchins and Bruland, 1998; Takeda, 1998) and on the stoichiometry of cultured diatoms (De La Rocha et al., 2000; Leynaert et al., 2004). Additionally, other studies showed that changes in elemental composition due to Fe stress were coupled to a decrease in cell size (Leynaert et al., 2004; Marchetti et al., 2007). In the case of Zn, its potential role in controlling primary productivity and the structure of phytoplankton communities is less well documented than Fe.

1.3 ROLE OF ZINC IN PHYTOPLANKTON NUTRIENT PHYSIOLOGY

A limited number of studies addressed the effects of Zn availability on phytoplankton nutrient physiology either in laboratory or field experiments. The following section describes our current knowledge of Zn distribution and speciation in marine waters, the physiological role of Zn in marine diatoms and its effects on macronutrients uptake and cellular elemental composition.

1.3.1 Concentrations and chemical forms of zinc in seawater

Total dissolved Zn concentrations increase between two to three orders of magnitude from oceanic to coastal and estuarine waters (Table 1.1). In oceanic surface waters (<50m deep), total dissolved Zn concentrations vary between 0.01 and 0.9 $x10^{-9}$ M (Bruland K., 1989; Ellwood and van den Berg, 2000; Lohan et al., 2002). In coastal and estuarine waters the range is from 0.06 to 230 $x10^{-9}$ M (van den Berg et al., 1987; Kozelka et al., 1998; Franck et al., 2003; Skrabal et al., 2006). In addition, total Zn concentration in seawater exhibits a nutrient-like vertical profile, where Zn is drawn down at the surface and regenerated at depth.

Total dissolved Zn concentrations include inorganic Zn (mainly Zn^{2+} and ZnCl) and Zn complexed to organic agents (Byrne et al., 1988; Sunda et al., 2005). Over 96% of Zn can be organically complexed in surface oceanic waters of the central North Pacific (Bruland K., 1989) and Northeastern Atlantic Ocean (Ellwood and van den Berg, 2000). In coastal and estuarine waters, the percentage of Zn-complexation can vary between 25% and 98% (Skrabal et al., 2006). The degree of Zn complexation in marine waters has important consequences for diatoms, since growth is dependent on the free Zn ion activity (Anderson et al., 1978). Thus, organic complexation in natural environment considerably reduces Zn availability for phytoplankton.

Table 1.1 – Concentrations of Zn in surface waters from open to nearshore waters.

Location	Total Zn	Zn^{2+}	References
Open Ocean	**($x10^{-9}$ M)**	**($x10^{-12}$ M)**	
North Pacific	0.01 – 0.34	n.a.	Bruland et al. (1979)
Central North Pacific (22-50m)	0.15 – 0.30	~ 2	Bruland (1989)
North East Pacific (10m)	0.04 – 0.90	n.a.	Lohan et al. (2002)
Northeastern Atlantic Ocean (3m)	0.28 – 0.72	6 – 20	Ellwood and van den Berg (2000)
Coastal, including continental slope	**($x10^{-9}$ M)**	**($x10^{-12}$ M)**	
Northeastern Atlantic Ocean (3m)	0.32 – 1.53	9.8 – 205	Ellwood and van den Berg (2000)
Eastern Tropical Pacific	0.06 – 0.10	n.a.	Franck et al. (2003)
Off Central California	0.07 – 0.10	n.a.	Franck et al. (2003)
Nearshore	**($x10^{-6}$ M)**	**($x10^{-9}$ M)**	
Scheldt estuary, Netherlands (Chlorinity: 4.8 – 14.26 ‰)	0.015 – 0.230	7.8 – 8.7	van den Berg et al. (1987)
Narragansett Bay, Rhode Island (Salinity: 24.9 – 30.3)	16 – 72	300 – 1300	Kozelka et al. (1998)
Cape River estuary, North Carolina (Salinity: 7 – 32)	≤5 – 67	n.a.	Skrabal et al. (2006)

Note: n.a. = data not available

1.3.2 Physiological role of zinc in the phytoplankton cell

Zinc has a critical role in different physiological pathways in phytoplankton. Zinc is a cofactor for the carbonic anhydrase (CA), alkaline phosphatase and 5'nucleotidase enzymes. Carbonic anhydrase catalyzes the interconversion of CO_2 and HCO_3^- and thus, has an important role in the acquisition of inorganic carbon and in the photosynthetic CO_2 concentration mechanisms (CCMs) (Badger and Price, 1994; Morel et al., 2002; Badger, 2003). The CCMs are an important adaptation of photosynthetic organisms to actively transport and accumulate inorganic carbon within the cell, and thus to aid carbon fixing by the enzyme RUBISCO (Badger, 2003). The enzymes alkaline phosphatase and 5'nucleotidase allow phytoplankton to access phosphorus contained in organic compounds by cleaving phosphate from phosphomonoesters or nuclotides, respectively (Shaked et al., 2006). Another important function of Zn is in the metabolism of DNA where it forms of Zn finger proteins (Da Silva and Williams, 1991).

Detailed studies of the Zn-enzyme systems in diatoms mainly focused on CA. As indicated above, CA catalyzes the interconversion of CO_2 and HCO_3^-, and it is essential for phytoplankton carbon acquisition. To perform its catalytic activity, the CA active site requires Zn as a co-factor. The role of Zn is to act as a Lewis acid accepting a pair of electrons and generating a hydroxide ion (base) that attacks CO_2 in a two-step catalytic mechanism (Badger, 2003). The general reaction catalyzed by the enzyme (E) CA is:

$$E\text{-}Zn^{2+}\text{-}OH^- + CO_2 <=> E\text{-}Zn^{2+} + HCO_3^-$$

The activity of carbonic anhydrase in the periplasmic and cytoplasmic spaces is well documented (Lane and Morel, 2000; Burkhardt et al., 2001). The activities of these

external and internal CAs are regulated by CO_2 and metal concentration (Morel et al., 2002). Under Zn-limiting conditions, Zn can be replaced by cobalt (Co) or cadmium (Cd) at the CA active site (Price and Morel, 1990). Moreover, experiments carried out with *Thalassiosira weissflogii* showed an important role of the silica frustule in providing a buffering environment for the extracellular CA activity (Milligan et al., 2002). Yet, to date the acquisition and concentration mechanisms of CO_2 in diatoms are not fully elucidated (Robert et al., 2007).

1.3.3 Zinc limitation in marine diatoms

The effect of Zn limitation on phytoplankton growth was first addressed in laboratory experiments with unialgal cultures. Anderson et al. (1978) showed that growth rate in *Thalassiosira weissflogii* was dependent on the concentration of the Zn ion activity, and they suggested that growth limitation would occur in unpolluted waters where organic complexation of Zn takes place. In addition, there is a difference in the Zn requirements between oceanic and coastal diatoms (Brand et al., 1983). Sunda and Huntsman (1992) looked at the relationships among Zn ion activity, cellular Zn and growth rate in the oceanic diatom *Thalassiosira oceanica* and the coastal diatoms *T. pseudonana* and *T. weissflogii*. They showed that oceanic species have the ability to reduce their internal Zn requirements to maintain maximum growth rates under low Zn^{2+} concentrations. A lower Zn requirement in oceanic diatoms is in agreement with lower Zn concentrations in oceanic waters compared to coastal waters (see Table 1; Brand et al., 1983).

Zn availability can also have an effect on the rate of $Si(OH)_4$ uptake. A decrease in $Si(OH)_4$ uptake rates at Zn-limiting concentrations was observed in *T. pseudonana*

(Rueter and Morel, 1981). Additionally, an interaction of copper (Cu) with the Zn-active site was suggested, since the rate of displacement of Zn depended on the ratio of Cu to Zn activities. These results indicated that $Si(OH)_4$ uptake could be mediated by a Zn dependent system, which is inactivated by Cu.

A recent study showed an effect of Zn (and Fe) limitation on the elemental cell quotas (C, N and Si) and biogenic silica production in the coastal diatom *T. weissflogii* (De La Rocha et al., 2000). In this study, Zn limitation increased C, N and Si content and the ratios Si/C and Si/N compare to those at Zn-replete conditions. In regards to Si production, Zn limitation resulted in a 60% decrease in maximum production rate and a 64% increase in the value of the half saturation constant (K_s) compare to Zn-replete conditions. The increase in K_s for Si uptake suggests that Zn is required for Si uptake, since the affinity of the transport system depended on Zn availability. Under low environmental $Si(OH)_4$ concentrations, differences in K_s at low Zn concentrations could affect the species composition of natural phytoplankton assemblages.

A few studies have addressed the effects of Zn during enrichment experiments in the field. These experiments indicated that Zn availability can affect the rates of macronutrient uptake and the community structure of phytoplankton assemblages in some regions of the oceans (Crawford et al., 2003; Franck et al., 2003; Leblanc et al., 2004). Zinc additions increased the maximum uptake rate (V_{max}) and decreased the K_s for $Si(OH)_4$ uptake in the high-nitrate, low-chlorophyll (HNLC) area off California (Franck et al., 2003). Yet, this study showed mixed effects of Zn on NO_3^- uptake kinetics. Also, the +Fe+Zn treatment showed a synergistic effect since +Fe+Zn addition increased V_{max} more than Fe alone (Franck et al., 2003).

In regards to the structure of natural phytoplankton assemblages, the first evidence of a strong effect of Zn availability was documented in the Sub-antarctic Zone near New Zealand (Leblanc et al., 2005). In this low silicate HNLC region, Zn additions changed the community structure from one dominated by the colonial-pennate diatom *Pseudo-nitzschia* sp. to one dominated by the solitary-pennate diatom *Cylindrotheca closterium.* In addition, Fe and Zn addition experiments in the Ross Sea and the Antarctic Circumpolar current along 170°W showed that Zn did not limit phytoplankton growth, but the +Fe+Zn treatments resulted in enhanced growth over Fe addition alone (Coale et al., 2003). Finally, results from Zn enrichment experiments in the oceanic Northeast Subarctic Pacific Ocean showed a slight but significant increase in chlorophyll *a*, an increase in the abundance of small diatoms and coccolithophores, and a decrease in dissolved HPO_4^{3-} and NO_3^- (Crawford et al. 2003). In this study, the +Fe+Zn treatment also exhibited an increase in the abundance of small diatoms and flagellates compared to +Fe treatment. All these studies point to an important role of Zn in phytoplankton nutrient physiology, productivity and community structure.

1.4 THESIS OBJECTIVES AND ORGANIZATION

The goal of this thesis was to examine the effects of Zn availability on growth rate, cell size, macronutrient uptake, elemental composition and stoichiometry in the coastal diatom *Skeletonema costatum* (Fig. 1.1) and the oceanic diatom *Thalassiosira oceanica* (Fig. 1.2). The term elemental refers to the macronutrients C, N, Si and P.

Laboratory experimentation with unialgal cultures is a valuable tool for estimating basic physiological parameters and responses at the species level under strictly controlled

conditions. The results from this study will allow us to make better predictions on the different physiological responses of coastal and oceanic diatoms to Zn limitation and the potential effects of Zn on nutrient ratios and phytoplankton assemblages in coastal and open ocean waters.

One coastal diatom (*Skeletonema costatum*) and one oceanic diatom (*Thalassiosira oceanica*) were used during this study. *Skeletonema costatum* is widely distributed in coastal regions around the world and there is extensive literature regarding its physiology and ecology. *Thalassiosira oceanica* has been the species of choice in previous trace metal studies. In the case of an oceanic diatom, Zn studies are challenging due to the very low Zn concentrations required to limit growth and therefore the relative easy of contamination of cultures. Experiments were done on acclimated cultures under strictly controlled trace-metal clean conditions to avoid contamination.

This thesis is organized in four chapters and three appendices. Chapter 1 presents a literature review and the objectives of the study. Chapter 2 describes the experimental design, culture conditions and the analytical methods used. Chapters 3 and 4 describe the results, and discussion and conclusions, respectively. Appendices A, B and C summarize the trace metal techniques employed and additional experiments performed during this thesis project.

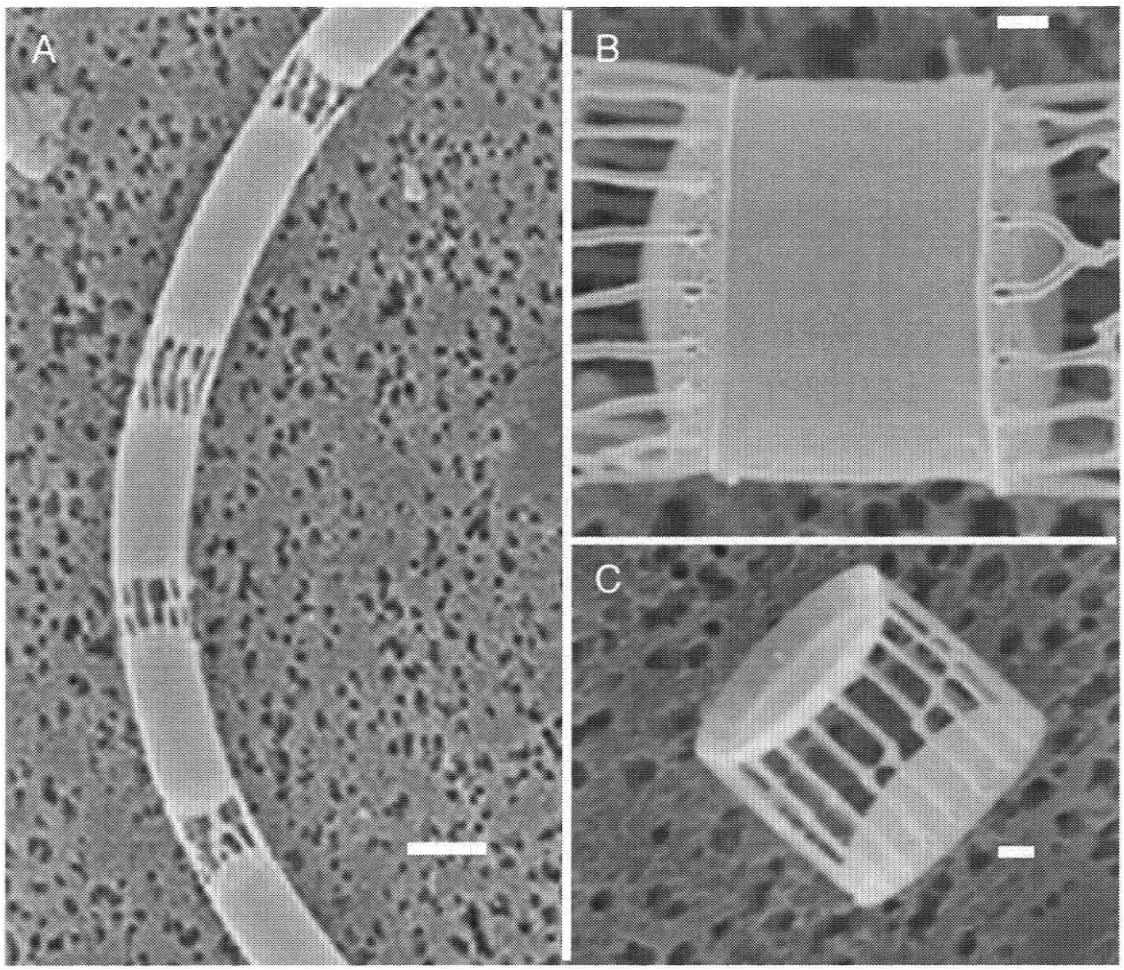

Fig. 1.1 Scanning electron micrographs of *Skeletonema costatum*: chain in girdle view (A, scale bar represents 5 μm), single cell (B) and detail of linking structures (C). Scale bar = 1 μm for (A) and (C).

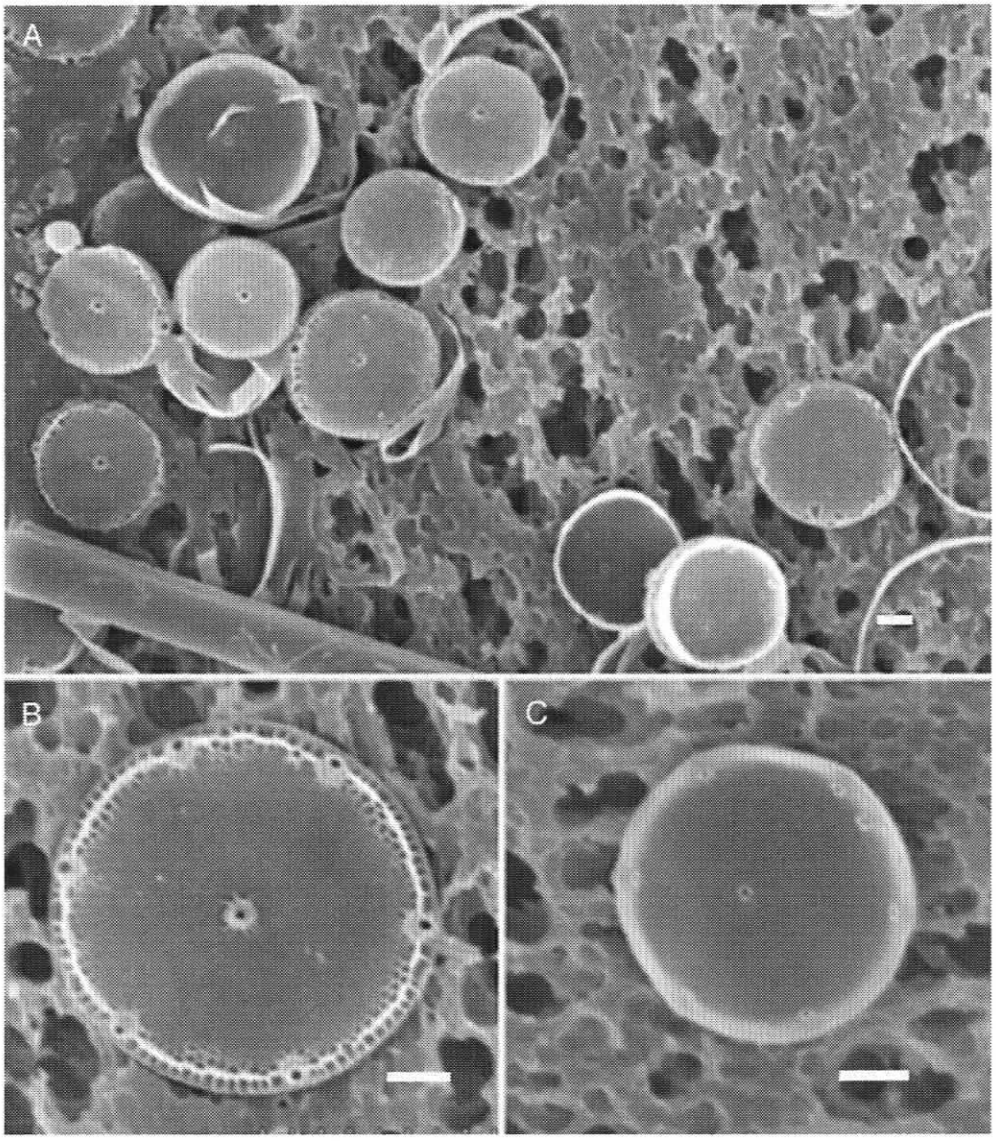

Fig. 1.2 Scanning electron micrographs of *Thalassiosira oceanica* (A), including outside view of valve (B) and internal view of valve (C). Scale bar = 1 μm.

CHAPTER 2 – MATERIALS AND METHODS

2.1 DIATOM SPECIES

The diatom species used in this study were *Skeletonema costatum* and *Thalassiosira oceanica* (see Figs. 1.1 and 1.2). The coastal diatom *S. costatum* was isolated from Saanich Inlet (British Columbia, Canada) in May 2006 and the oceanic diatom *T. oceanica* (NPCC 610, clone 13-1) was purchased from the Canadian Center for the Culture of Microorganisms (Department of Botany, University of British Columbia). *Thalassiosira oceanica* was originally isolated from the Sargasso Sea in December 1958 (North Atlantic).

2.2 CULTURE MEDIA

Diatoms were grown in semi-continuous unialgal cultures with natural seawater from station PAPA (OSP, at 50°N latitude; 145°W longitude) in the Northeast Subarctic Pacific Ocean (an HNLC region with low metal concentrations). Seawater was collected using trace metal clean (TMC) techniques from 10-15 m and brought into a Laminar Flow Clean bench with Teflon Bellow pump. Seawater was filtered through a 0.2 µm OPTICAP filter and stored in doubled-bagged acid-cleaned carboys. Once in the laboratory, carboys were kept in the dark and in a TMC enclosure.

Culture media were prepared by meticulously following TMC techniques (see Appendix A for details). First, macronutrients were added to OSP seawater to a final concentration of 100 µM NO_3^-, 100 µM $Si(OH)_4$ and 10 µM HPO_4^{2-}. Media was then passed through a polypropylene column with Chelex 100 resin and collected in acid

clean polycarbonate bottles. A Chelex 100 resin was employed to remove background metals in seawater and metal impurities in nutrients reagent; all steps were performed in a Polypropylene Vertical Laminar Flow Clean Bench (Microzone Corporation). The chelexed media was microwave sterilized (Keller et al., 1988) and allowed to cool in the Clean Bench. After cooling, filter-sterilized EDTA-trace metal (without Co and Zn), and vitamin solutions were added to the media in accordance to Aquil concentrations (Price et al., 1988/1989; Sunda et al., 2005) (see Appendix A). Zn was then added to the media from a filter-sterilized stock solution. Finally, the media was allowed to chemically equilibrate overnight and was stored in double-bag polycarbonate (PC) bottles in a TMC enclosure.

The TMC enclosure employed during this study consisted in a plastic tent with positive pressure provided by a plastic Air Cleaner with a HEPA filter of plastic construction.

2.3 CULTURE CONDITIONS

Experimental unialgal cultures were grown in acid-clean PC vessels at 20°C using a light: dark cycle of 14:10 h. Photosynthetically active radiation (PAR) was 200 µmol photons m^{-2} s^{-1} for *S. costatum* and 240 µmol photons m^{-2} s^{-1} for *T. oceanica*. Optimal PAR for each species was determined from additional experiments that addressed the effects of irradiance on growth rates (see Appendix B). Cultures were maintained at the appropriate conditions using the semi-continuous culture technique (MacIntyre and Cullen, 2005). Cells were grown and allowed to acclimate to culture conditions for at least 10 generations before the start of any experimental work.

2.4 EXPERIMENTAL DESIGN

Two different types of experiments were performed during this thesis.

The first set of experiments was designed to determine the **effects of Zn availability on growth rate and cell morphology.** Triplicate cultures of each species were grown in acid-clean 28 ml PC tubes at different total Zn concentrations in the range of 15.8 to 79.7 $x10^{-9}$ M for *S. costatum* and 1.59 to 79.7 $x10^{-9}$ M for *T. oceanica*. Table 2.1 shows the chemical Zn speciation in the media calculated using MINEQL+ (Westall, 1976). *In vivo* fluorescence was measured daily at the same time to follow culture growth. Once cells were grown for at least 10 generations under each set of culture conditions (e.g. at different Zn concentrations), growth rates were calculated by using the relative changes *in vivo* fluorescence over time. Cell size measurements were performed on samples collected during the exponential growth phase (see below).

The second set of experiments was designed to determine the **effect of Zn limitation on the elemental composition and macronutrient incorporation.** Triplicate cultures of *S. costatum* and *T. oceanica* were grown in acid-clean double-bag 2-L PC round bottles at Zn-replete and at Zn-limiting conditions. Zn-replete cultures of both species had a Zn^{2+} concentration of 13 $x10^{-12}$ M. Zn-limiting cultures had a Zn^{2+} concentration of 3.47 $x10^{-12}$ M for *S. costatum* and 0.26 $x10^{-12}$ M for *T. oceanica*. These Zn^{2+} concentrations were chosen based on the first set of experiment. Cells were acclimated to the culture conditions for at least 10 generations before sampling. Each culture was sampled during three consecutive days at exponential growth phase for the determination of dissolved nutrients (NO_3^-, $Si(OH)_4$ and HPO_4^{2-}), biogenic silica, particulate organic carbon, nitrogen and phosphorus, chlorophyll *a*, cell counts and cell

size measurement. Samples were collected for both species at the same time every day to avoid diel changes in the cell physiology due to the light: dark cycle. The methods used for the determination of each parameter are described below. Culture sampling and manipulation were performed in the Laminar Flow Clean bench at all times.

2.5 DETERMINATION OF CELL SIZE MEASUREMENTS

A 10-ml sample obtained at exponential growth phase from each culture was preserved with 600 µl of 25% glutaraldehyde for the determination of cell size parameters. Cell size parameters included cell diameter, cell length (for *S. costatum*), cell height (for *T. oceanica*), cell surface, cell volume and cell surface to volume ratio (S/V). For every experimental treatment, mean values were obtained by measuring > 25 cells in *S. costatum* and >15 cells in *T. oceanica.* Differences in cell size measurements among Zn conditions were statistical analyzed with one-way ANOVA.

Cell diameter, cell length and cell height were determined with an Olympus IX71 epifluorescence inverted microscope. Cell surface and cell volume were estimated by using geometrical shapes that resemble the shape of each species. In this study, the geometric models proposed by Sun and Liu (2003) were employed.

Table 2.1 Chemical Zn speciation in the culture media calculated with MINEQL+ software for *Skeletonema costatum* and *Thalassiosira oceanica.*

Total Zn ($x10^{-9}$ M)	Zn^{2+} ($x10^{-12}$ M)	pZn (= -log[Zn^{2+}])
S. costatum		
79.7	13.1	10.88
39.8	6.02	11.22
31.9	5.25	11.28
27.1	4.47	11.35
20.8	3.47	11.46
15.8	2.63	11.58
T. oceanica		
79.7	13.1	10.88
39.8	6.02	11.22
15.8	2.63	11.58
3.19	0.52	12.28
1.59	0.26	12.58

For *S. costatum*, cell volume (V) and cell surface area (S) were calculated assuming a shape composed of one cylinder with 2 half spheres, and using equations 1 and 2, respectively:

$$V = \pi \cdot b^2 \cdot (a/4 - b/12) \qquad (1)$$

$$S = \pi \cdot a \cdot b \qquad (2)$$

where 'a' is the cell length and 'b' is the diameter in girdle view (Fig. 2.1A).

For *T. oceanica*, cell volume (V) and cell surface area (S) were calculated assuming a cylindrical shape, and using equations 3 and 4, respectively.

$$V = \pi/4 \cdot a^2 \cdot c \qquad (3)$$

$$S = \pi \cdot a \cdot (a/2 + c) \qquad (4)$$

where 'a' is the diameter and 'c' is the pervalvar axis length in girdle view (Fig. 2.1B).

2.6 SCANNING ELECTRON MICROGRAPHS

Preserved *S. costatum* was observed with a Hitachi S-3500N Scanning Electron Microscope (Department of Biology, Electron Microscope Facilities). To remove organic matter, samples were treated with an acid mixture (1:1:3, sample:HNO_3:H_2SO_4), boiled for up to 1 minute and then filtered onto a 0.65 μm PC filter. Samples were then rinsed with distilled water and dehydrated in ethanol series. Filters were kept in a desicator until they were mounted on stubs and sputter coated with gold-palladium. Micrographs were taken with a Hitachi S-3500N SEM, AMT 2k x 2K CCD camera.

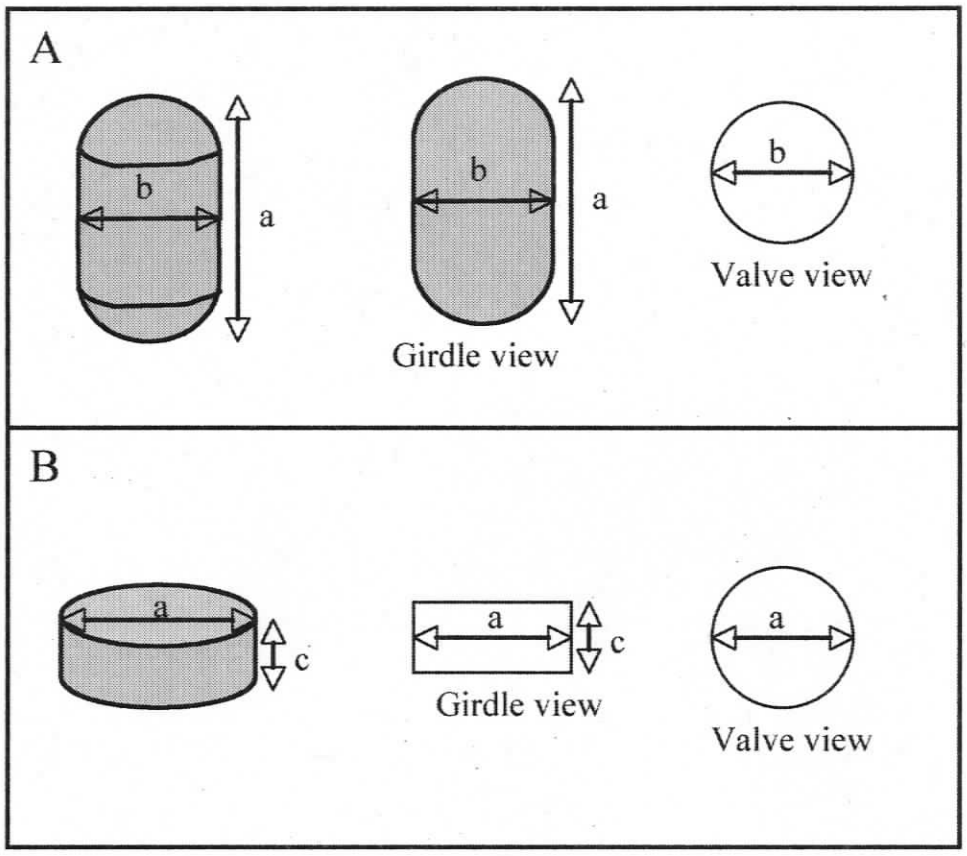

Fig. 2.1. Geometrical shapes used for the calculation of cell surface and cell volume in *Skeletonema costatum* (A) and *Thalassiosira oceanica* (B) (adapted from Sun and Liu, 2003). *S. costatum* resembles a geometrical shape composed of one cylinder with 2 half spheres, where 'a' is the cell length and 'b' is the diameter. *T. oceanica* resembles a cylindrical shape, where 'c' is the pervalvar axis length and 'a' is the diameter.

2.7 CHEMICAL ANALYSIS

The following section includes a description of the chemical analysis performed during this study.

2.7.1 Dissolved nutrients

Samples (30 ml) were filtered through 0.7-µm precombusted glass fibre filters for dissolved nutrient analysis. The filtrates were collected into acid clean polypropylene bottles and stored at -20°C until analysis. Dissolved NO_3^-, $Si(OH)_4$ and HPO_4^{2-} concentrations were measured with an Astoria-Pacific Nutrient Autoanalyzer following Barwell-Clarke and Whitney (1996).

2.7.2 Chlorophyll *a*

Samples (30 to 40 ml) were filtered through 0.7-µm glass fiber filters for chlorophyll *a* (Chl-*a*) extraction and determination following the procedure outlined in Parsons et al. (1984). Filters were stored at -20 °C until further analysis. Aqueous acetone (90%) was added to the filters, followed by a 10-minute sonication period and samples were subsequently kept at -20 °C for 24h. *In vitro* chlorophyll fluorescence was measured with a Turner Designs 10-AU fluorometer. Chl-*a* cellular quotas were normalized per cell volume (fg Chl-*a* μm^{-3}).

2.7.3 Biogenic Silica

Biogenic silica (BSi) was determined following a modified version of Brezezinski and Nelson (1986). Samples (10 to 40 ml) were filtered through 0.6-µm polycarbonate

filter. Filters were placed in 15-ml polypropylene tubes and dried at 60°C for approximately 48 h. Dried filters were digested for 1 h with 4 ml of 0.2 N NaOH in a 95°C water bath. Samples were cooled and neutralized with 1 ml of 1N HCl. The $Si(OH)_4$ concentration of the digest was measured with a DU530 Beckman UV/Vis spectrophotometer at 810 nm.

Biogenic silica quotas were normalized per cell number (pmol BSi $cell^{-1}$), per cell surface area (fmol BSi μm^{-2}) and per cell volume (fmol BSi μm^{-3}).

2.7.4 Particulate organic nitrogen and carbon

Samples (20 to 40 ml) were filtered through 0.7-µm pre-combusted glass fibre filters and dried at 60°C for 48 h. Particulate organic carbon (POC) and nitrogen (PON) were measured with a PDZ Europa ANCA-GSL elemental analyzer interfaced to a PDZ Europa 20-20 isotope ratio mass spectrometer (PDZ Europa, Northwich, UK) at the University of California, Davis, Stable Isotope Facility.

POC and PON quotas were normalized per cell number (pmol POC or PON $cell^{-1}$) and per cell volume (fmol POC or PON μm^{-3})

2.7.5 Particulate organic phosphorus

Particulate organic phosphorus (POP) was determined by wet-oxidation following the procedure outlined by Pujo-Pay and Raimbault (1994). Samples (20 to 40 ml) were filtered through 0.7-µm pre-combusted glass fibre filters, and filters were kept at -20 °C until analysis. Digestion was carried out by placing the filters into 50 ml glass tubes containing 2.5 ml of oxidising reagent and 20 ml of water. The oxidising reagent consisted of 15 g of potassium persulfate and 7.5 g of boric acid diluted in 70 ml of 1.5M

NaOH solution, and made up to a final volume of 250 ml with Milli-Q water. Tubes were tightly closed and autoclaved at 120°C for 30 minutes. After the digestion period, phosphate concentrations were determined spectrophotometrically following Parson et al. (1984).

POP quotas were normalized per cell number (pmol POP $cell^{-1}$) and per cell volume (fmol POP μm^{-3}).

2.8 CALCULATION OF GROWTH RATES

Growth rates were calculated from changes of *in vivo* fluorescence and cell numbers over time. *In vivo* fluorescence was measured daily at the same time during the whole course of the experiments. Samples for cell numbers (5 ml) were also collected at the same time and preserved with lugol's iodine solution. Cell enumeration was performed with an Olympus IX71 epifluorescence inverted microscope using a Rafter-Sedgwick chamber for *S. costatum* and a hemacytometer for *T. oceanica.* The use of *in vivo* fluorescence as a proxy of cell growth was tested for both species (regressions between *in vivo* fluorescence and cell numbers were $r^2 > 0.95$ for each species, data not showed).

Growth rates (μ) as a function of Zn concentration (S) were fitted with a Monod model [$\mu = \mu_{max}$ (S / ($K_{s\text{-}Zn}$+S))], allowing the calculation of the half-saturation constant ($K_{s\text{-}Zn}$) and maximum growth rate (μ_{max}). In the case of *S. costatum,* a modified version of Monod [$\mu = \mu_{max}$ ((S-S_{min}) / ($K_{s\text{-}Zn}$+S- S_{min}))] was used, where S_{min} represents the Zn concentration at which *S. costatum* did not exhibit growth (Kovarova et al., 1996).

2.9 CALCULATION OF ELEMENTAL QUOTAS, ELEMENTAL RATIOS AND INCORPORATION RATE OF MACRONUTRIENTS

Elemental quotas were determined by measuring the particulate concentration of each element (C, N, Si and P), and then normalizing these values by cell number and cell surface or cell volume. The following molar ratios were then calculated: C:N, Si:C, Si:N, C:P and N:P. Differences between Zn-replete and Zn-limiting conditions in elemental quotas and ratios were statistical analyzed with t-tests.

The incorporation rate of each macronutrient into the cells was calculated over a 24 h period from the increase in BSi, PON, POC or POP in the medium, and then divided by the average cell number over the same period. The incorporation rates were then normalized per cell volume (e.g fmol BSi μm^{-3} d^{-1}) or cell surface (e.g. fmol BSi μm^{-2} d^{-1}). Differences in incorporation rates of macronutrients between Zn-replete and Zn-limiting conditions were statistical analyzed with t-tests.

CHAPTER 3 - RESULTS

The results of this study are divided into two sections. Section 3.1 addresses the variation of growth rates and cell morphology with Zn availability in *S. costatum* and *T. oceanica* (experiment 1). Section 3.2 describes the effects of Zn limitation on the elemental composition and stoichiometry of the two diatoms (experiment 2).

3.1 – EFFECT OF ZN AVAILABILITY ON GROWTH RATE AND CELL MORPHOLOGY IN *SKELETONEMA COSTATUM* AND *THALASSIOSIRA OCEANICA*

3.1.1 Variations in growth rates from Zn-limiting to Zn-replete conditions

In this section, growth rates were calculated from changes in *in vivo* fluorescence over time. Growth rates of *S. costatum* decreased three times from Zn-replete to Zn-limiting conditions (13.1 $x10^{-12}$ M - 3.5 $x10^{-12}$ M Zn^{2+}) (Fig. 3.1). The maximum specific growth rate (μ_{max}) was 1.25±0.04 d^{-1} (mean ± 1SE), and it decreased sharply below [Zn^{2+}] ≤ 6 $x10^{-12}$ M. *S. costatum* did not grow at Zn^{2+} concentrations ≤ 2.63 $x10^{-12}$ M. Growth rates as function of Zn concentrations were modeled with a modified version of the Monod model (Kovarova et al., 1996). The 95% confidence intervals were μ_{max} = 1.44 ±0.13 d^{-1} and $K_{s\text{-}Zn}$ = 4.07 $x10^{-12}$ ± 4.15$x10^{-13}$ Zn^{2+} M. The 95% confidence interval for the minimum Zn^{2+} concentration for growth (S_{min}) was 2.64 $x10^{-12}$ ±8.27 $x10^{-14}$ M.

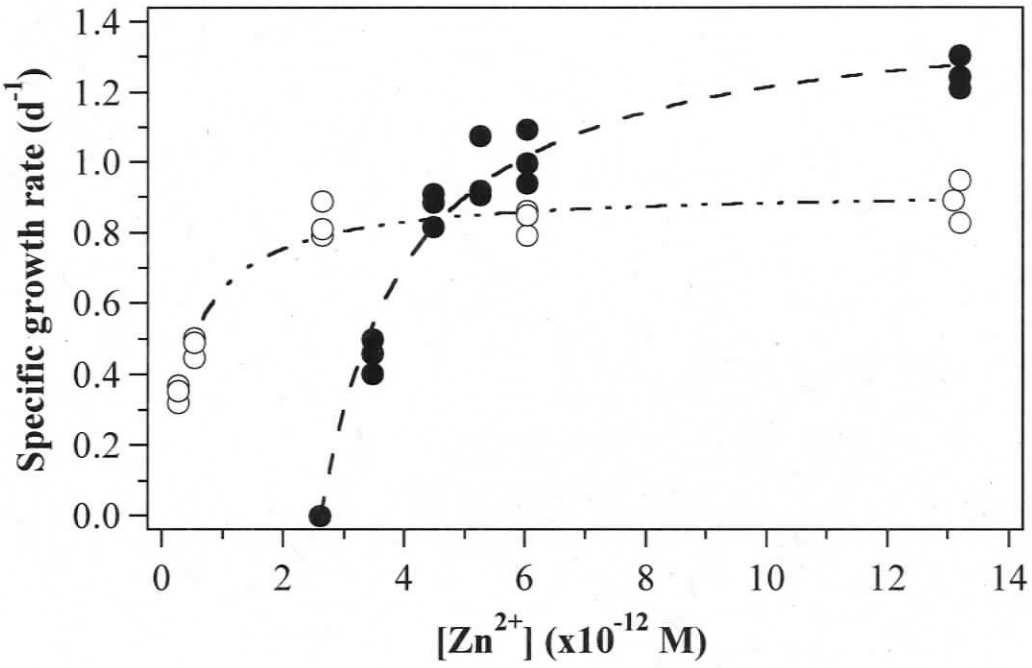

Fig. 3.1. Specific growth rates (μ) in (●) *Skeletonema costatum* and (○) *Thalassiosira oceanica* at increasing Zn^{2+} concentrations. The curves represent non-linear fits to the Monod model for *T. oceanica* (- –) and to a modified version of the Monod model for *S. costatum* (– –), See Materials and Methods for explanation on the modified version of the Monod model.

In the case of *T. oceanica,* growth rates decreased two and a half times from Zn-replete to Zn-limiting conditions. The μ_{max} was 0.89 ±0.03d^{-1} (mean ± 1SE) and it was achieved at concentrations ≥ 2.6x10^{-12} M [Zn^{2+}] and remained constant to 13.1x10^{-12} M [Zn^{2+}]. *T. oceanica* exhibited growth at all the Zn^{2+} concentration tested and the μ decreased only at Zn^{2+} < 2.6 x10^{-12} M. Growth rates of *T. oceanica* as a function of Zn concentrations were fit to a Monod model. The 95% confidence intervals were μ_{max} = 0.92 ±0.04 d^{-1} and $K_{s\text{-}Zn}$ = 4.46 x10^{-13} ± 9.65x10^{-14} Zn^{2+} M. Overall, the oceanic diatom achieved maximum growth rates at Zn concentrations at which *S. costatum* already exhibited a severe reduction in growth.

3.1.2 Variations in cell morphology at different Zn concentrations

Cell surface area and cell volume were the parameters used to describe cell morphology (also referred to as cell size) in this study. In general, cultures of the coastal diatom *S. costatum* were composed of chains of cylindrical cells joined by extracellular silica rods. In this species, there was a significant effect of increasing Zn concentrations on cell size parameters (Fig. 3.2). Both cell volume and cell surface and significantly increased with increasing Zn concentrations (one-way ANOVA, $p<0.01$) (Fig. 3.2A and B). Cell volume increased four times from the lowest Zn^{2+} concentration (3.5 x10^{-12} M) to Zn-replete conditions, but surface area increased only two–fold. As a result, there was a 45% reduction of cell surface area to cell volume ratio (S/V) from 1.35 ±0.09 (mean ± 1SE) at the lowest Zn concentration to 0.74 ±0.09 (mean ± 1SE) in Zn-replete cells (one-way ANOVA, $p<0.01$). Cell diameter in *S. costatum* increased from 3.31 ±0.35 μm (mean ± 1SE) at the lowest Zn concentration to 10.72 ±0.32 μm (mean ± 1SE) at Zn-

replete cultures. In comparison, cell length significantly decreased with Zn concentrations from 12.66 ±0.20 μm at the lowest Zn concentration (mean ± 1SE) to 8.03 ±0.12 μm (mean ± 1SE) at Zn-replete conditions (one-way ANOVA, $p<0.01$). An additional feature observed under the microscope was that the number of cells per chain decreased in Zn-limiting compared to Zn-replete cultures (data not shown). In summary, cultures of *S. costatum* showed longer and narrower cells under Zn-limiting conditions, while Zn-replete cultures presented wider and shorter cells with a larger number of cells per chain (Fig. 3.3).

Since Zn availability affected growth rates and cell morphology in *S. costatum* the relationship between these two variables was further explored. The relative growth rates were calculated as μ/μ_{max}, where μ represents the specific growth rates at each Zn^{2+} concentration and μ_m is the maximum growth rate estimated from the modified version of Monod model. Variations in cell morphology and relative growth rates exhibited a strong linear correlation ($0.8\leq |r| \leq 1$), as indicated by the correlation coefficient (r) between μ/μ_m and cell volume ($r = 0.91$), cell surface ($r = 0.89$), S/V ratio ($r = -0.93$), cell diameter ($r = 0.91$), and cell length ($r = -0.71$) (Fig. 3.4). The linear relationships between cell size and relative growth rates suggest that both respond similarly to Zn limitation.

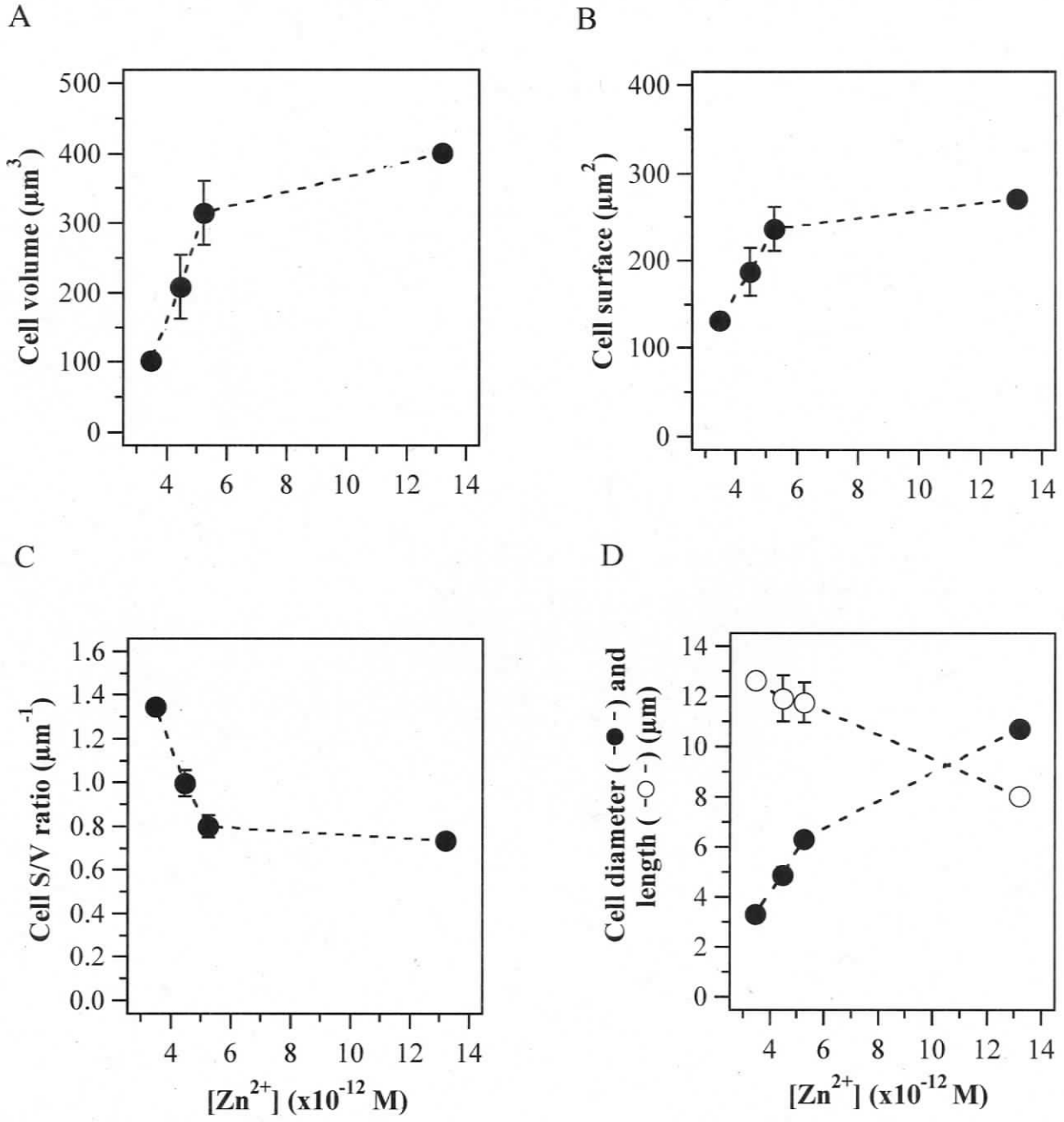

Fig. 3.2 Cell volume (A), cell surface (B), cell surface to volume ratio (S/V ratio) (C), and cell diameter and length (D) as a function of Zn^{2+} concentrations in *Skeletonema costatum*. Symbols represent the mean ± 1SE of triplicate cultures. When error bars are not visible, they are smaller than the symbol.

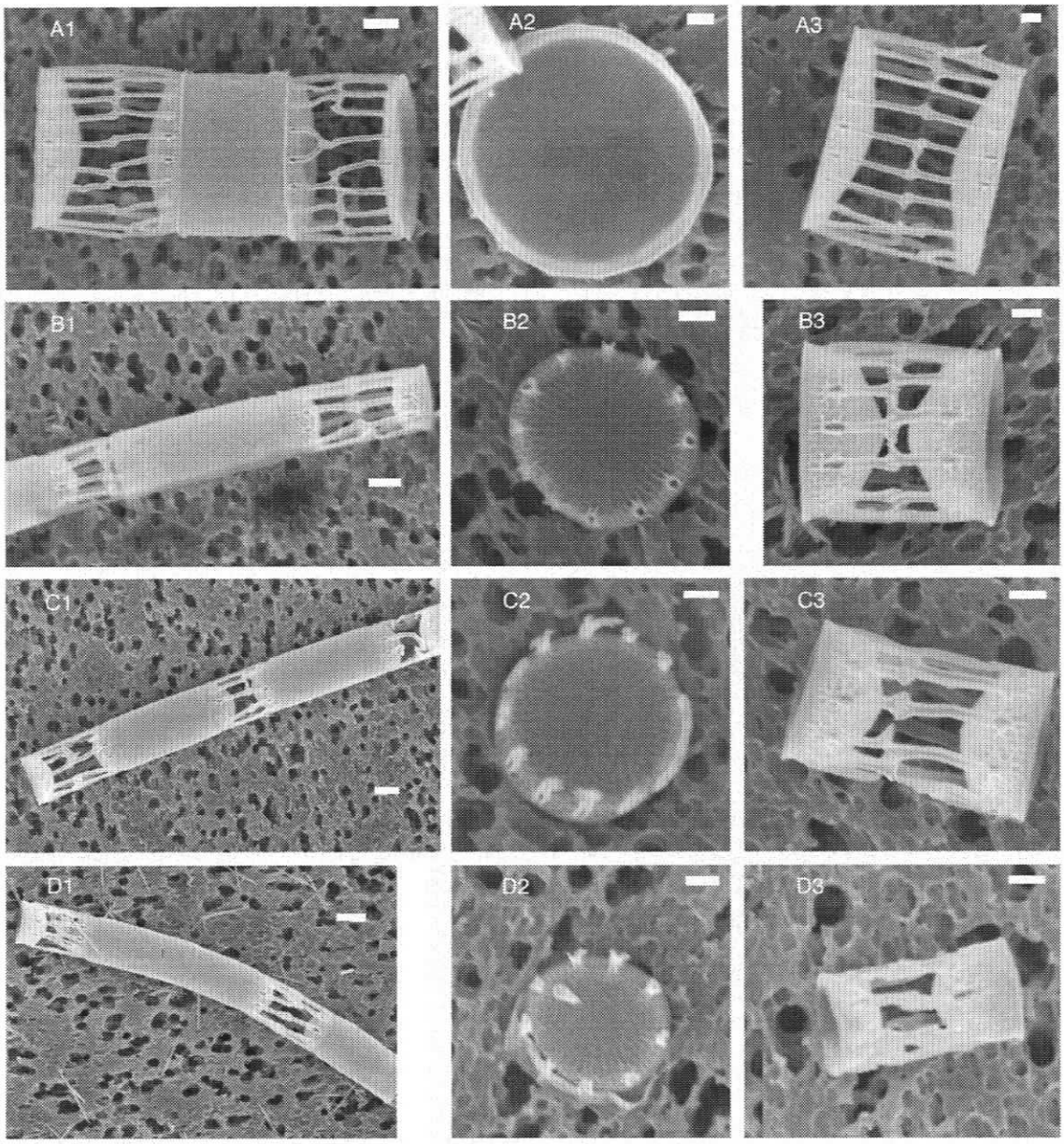

Fig. 3.3. Scanning electron micrographs of *Skeletonema costatum* at different Zn^{2+} concentrations: $13.18x10^{-12}$ M (A1-A3), $6.02x10^{-12}$ M (B1-B3), $4.46x10^{-12}$ M (C1-C3) and $3.46x10^{-12}$ M (D1-D3). Chains in girdle view (A1, B1, C1 and D1; scale = 2 μm), valve view (A2, B2, C2 and D2) and detail of linking structures (A3, B3, C3 and D3). Scale bar is 1 μm unless otherwise indicated.

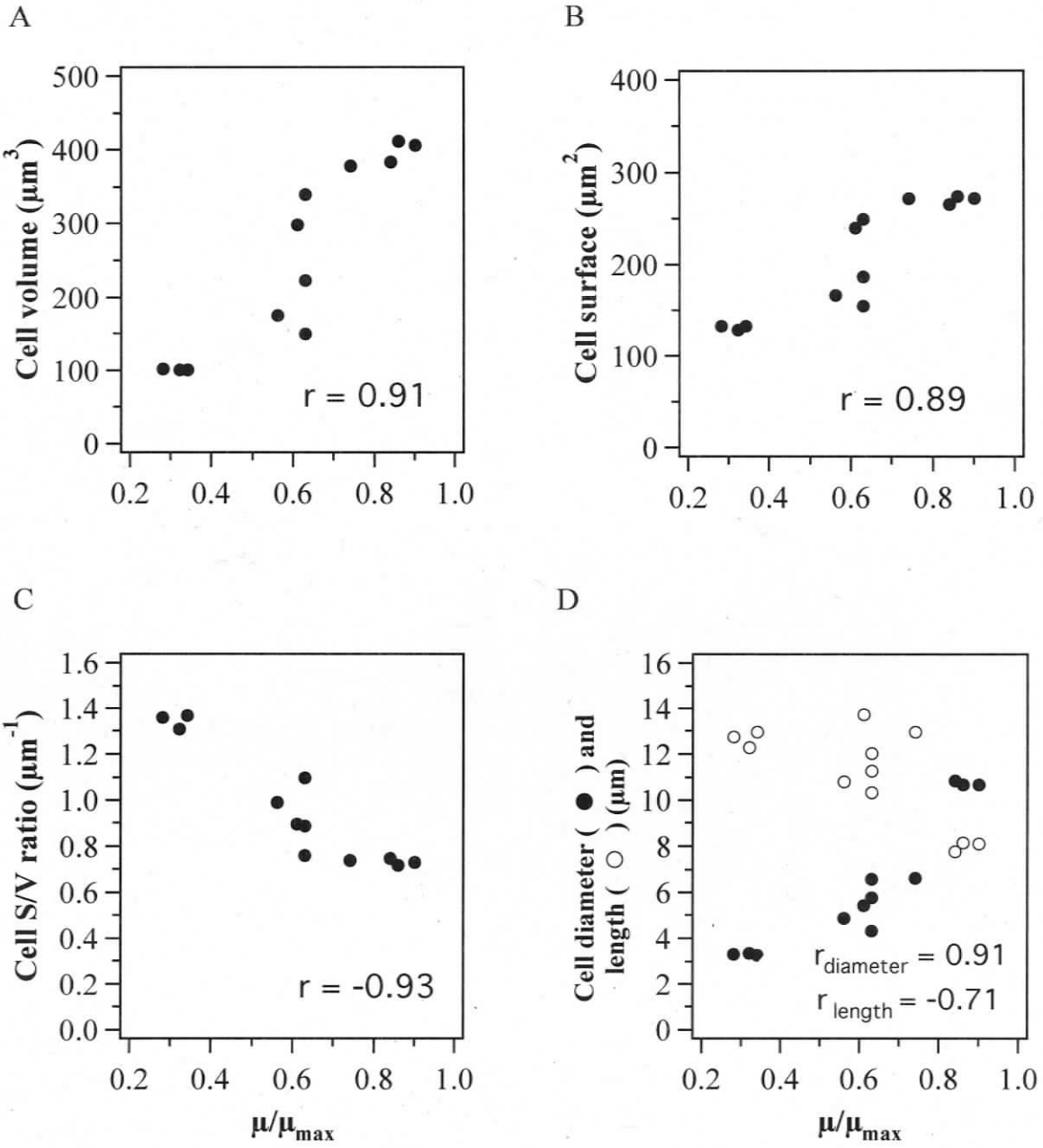

Fig. 3.4 Cell volume (A), cell surface (B), cell S/V ratio (C), and cell diameter and cell length (D) as a function of relative growth rate (μ/μ_{max}) in *Skeletonema costatum*. The r is the correlation coefficient, μ represents the specific growth rates at each Zn^{2+} concentration and μ_{max} is the maximum growth rate estimated from the non-linear modified version of the Monod model. Symbols represent mean values of at least 25 cells for culture.

Cultures of *T. oceanica* were composed of solitary cells of cylindrical shape in which cell diameter was longer than the cell pervalvar axis. Unlike *S. costatum*, the oceanic diatom did not show significant increasing or decreasing trends in cell morphology with Zn concentrations (Fig. 3.5). The cell size parameters (cell volume, surface, S/V ratio, diameter, and pervalvar axis) did not exhibit significant differences with Zn concentrations (one way ANOVA, $p>0.01$). Thus, cell size in the oceanic diatom was independent of the Zn condition.

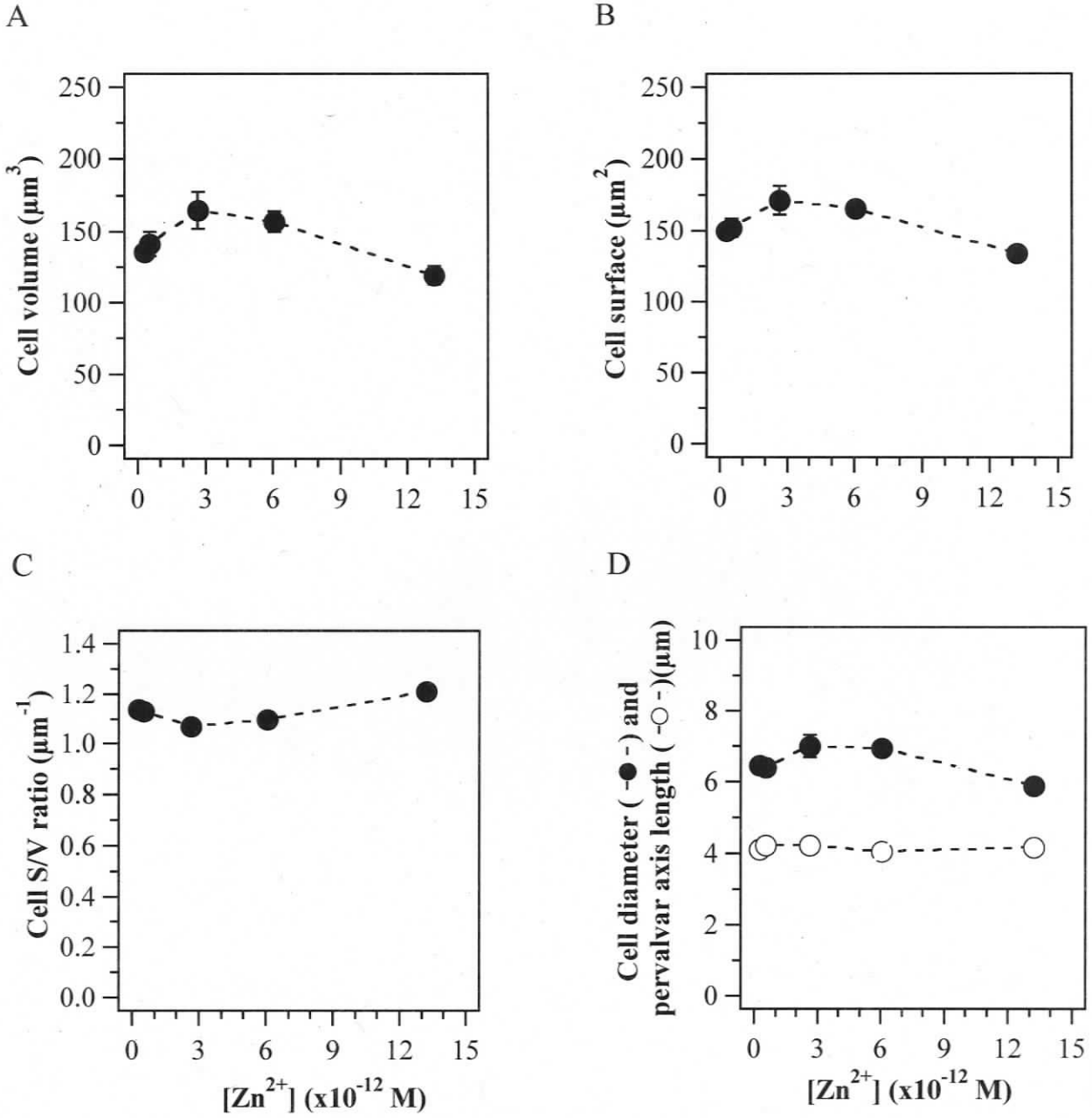

Fig. 3.5. Cell volume (A), cell surface (B), cell S/V ratio (C) and cell diameter and pervalvar axis (D) as a function of Zn^{2+} concentrations in *Thalassiosira oceanica*. Symbols represent the mean ± 1 SE of triplicate cultures. When error bars are not visible, they are smaller than the symbol.

3.2 EFFECT OF ZN LIMITATION ON ELEMENTAL COMPOSITION AND INCORPORATION OF MACRONUTRIENTS IN *SKELETONEMA COSTATUM* AND *THALASSIOSIRA OCEANICA*

The effect of Zn limitation on elemental quotas and ratios in diatom cultures was investigated under one Zn-replete and one Zn-limiting treatment for each species. Cultures of *S. costatum* were exposed to the following two Zn treatments: 13.1 $x10^{-12}$ M Zn^{2+} (Zn-replete) and 3.5 $x10^{-12}$ M Zn^{2+} (Zn-limiting). The Zn treatments for *T. oceanica* were 13.1 $x10^{-12}$ M Zn^{2+} (Zn-replete) and 0.26 $x10^{-12}$ M Zn^{2+} (Zn-limiting).

This section presents an analysis of the growth rates, elemental quotas and ratios, and macronutrient incorporation rates under Zn-replete and Zn-limiting conditions.

3.2.1 Growth rates at Zn-limiting and Zn-replete conditions

In this experiment, growth rates were calculated both by changes in *in vivo* fluorescence and cell numbers over time. In *S. costatum*, growth rates based on *in vivo* fluorescence were 1.48 ±0.02 d^{-1} (μ_m) in Zn-replete cultures and 0.57 ±0.03 d^{-1} (mean ± 1SE) (38% of μ_m) in Zn-limited cultures. Growth rates in *T. oceanica* were 0.96 ±0.06 d^{-1} (mean ± 1SE) (μ_m) in Zn-replete cultures and 0.39 ±0.06 d^{-1} (mean ± 1SE) (40% of μ_m) in Zn-limited cultures. Growth rates calculated by cell numbers were not significantly different from those calculated by *in vivo* fluorescence (t-test, $p>0.01$).

In addition to the effects on growth rate, nutrient limitation can also affect maximum yield (i.e., the amount of final biomass). During these experiments, yield limitation was evident only for the coastal diatom (Fig. 3.6). Cell numbers at stationary

phase of growth resulted in a final value of 2.29 ±0.31 x 10^5 cells/mL (mean ± 1SE) in Zn-replete cultures versus 1.61 ±0.05 x 10^5 cells/mL (mean ± 1SE) in Zn-limited cultures, representing a decrease of 30% under Zn limitation. Yield limitation could also be occurring in *T. oceanica*, but these cultures did not plateau during the experimental period.

3.2.2 Chlorophyll *a* quotas

The chlorophyll *a* (Chl-*a*) quota (or content) in both diatoms species was assessed at Zn-limiting and Zn-replete conditions. In *S. costatum*, chl-*a* quotas normalized to cell volume decreased by 20% under Zn limitation, but this result was significant only at $p<0.05$ (Fig. 3.7A). The ratio of Chl-*a* to C content also decreased significantly (~ 45%) from 0.169 ±0.001 mmol:mol (mean ± 1SE) at Zn-replete conditions to 0.091 ±0.005 mmol:mol (mean ± 1SE) at Zn-limiting conditions (t-test, $p<0.01$) (Fig. 3.7B).

In *T. oceanica,* Chl-a content per cell volume also decreased by 20% at Zn limiting concentrations, but the difference was not statistically significant ($p>0.01$) (Fig. 3.7A). In *T. oceanica*, there was no change in the Chl-*a* to C content ratio between Zn-replete and Zn-limiting conditions (t-test, $p>0.01$), with mean values ± SE of 0.125 ±0.005 mmol:mol and 0.115 ±0.006 mmol:mol, respectively (Fig. 3.7B).

In summary, Zn availability affected the Chl-*a* content in both species, although Chl-*a* to carbon content ratio exhibited differences only in the coastal diatom.

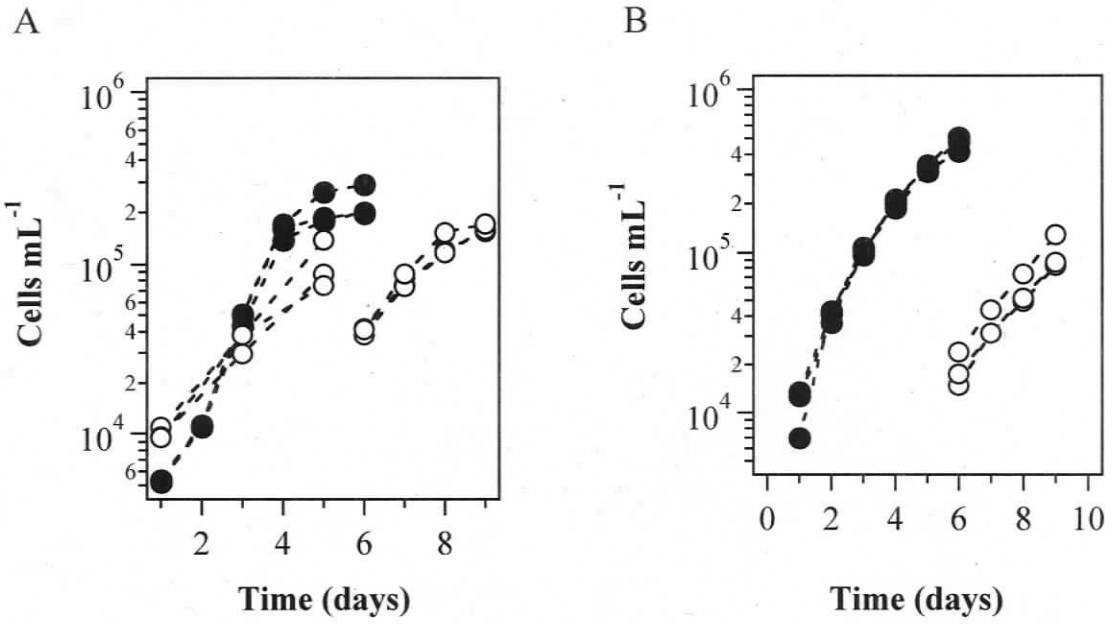

Fig. 3.6 Changes in cells numbers as a function of time at (●) Zn-replete and (○) Zn limiting conditions for triplicate cultures of *Skeletonema costatum* (A) and *Thalassiosira oceanica* (B).

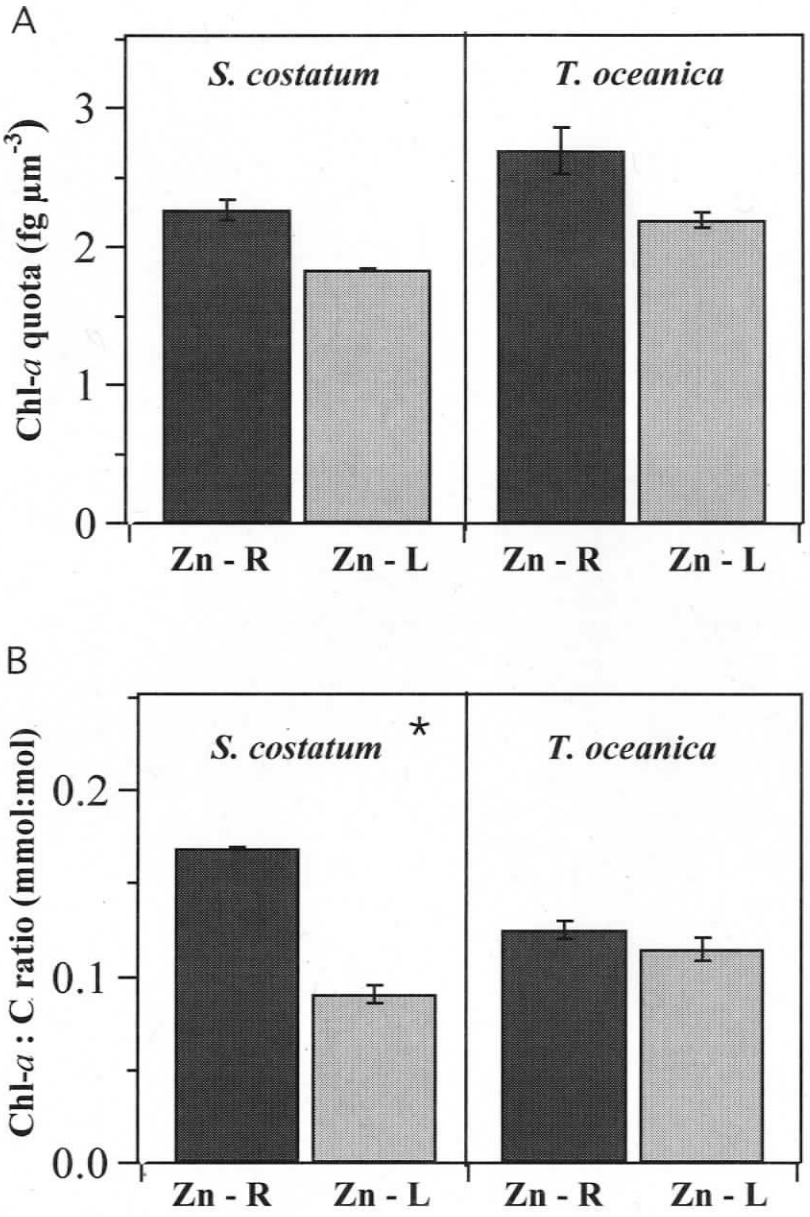

Fig. 3.7 Chlorophyll *a* content per cell volume (A), and chlorophyll *a* to carbon content ratio (B) at Zn-replete (Zn–R) and Zn-limiting (Zn–L) conditions in *Skeletonema costatum* and *Thalassiosira oceanica*. Bars represent the mean ± 1 SE of triplicate cultures. * Indicates significant change in Chl-*a*: C ratio between the two Zn treatments (t-test, $p<0.01$).

3.2.3 Elemental composition and ratios

Elemental quotas:

In *S. costatum*, C, N, Si and P quotas (or content) per cell decreased between two and four times from Zn-replete to Zn-limiting conditions (Table 3.1). Since there is a large difference in cell volume and surface area between Zn-replete and Zn-limited conditions, and to ensure a good comparison between Zn treatments, elemental quotas were normalized per cell volume. Si was also normalized per unit of cell surface (Si_S) (Brzezinski, 1985). Under Zn limitation, C content per cell volume significantly increased by 52% (t-test, $p<0.01$) (Table 3.1 and Fig. 3.8A). Unlike C content, N content (per cell volume) did not vary with Zn availability (t-test, $p>0.01$). Si content per cell volume decreased 20% under Zn limitation, but differences were not significant (t-test, $p>0.01$). However, Si content per surface area significantly decreased by 50% under Zn limitation (t-test, $p<0.01$). Phosphorus content per cell volume significantly increased by 55% under Zn limitation (t-test, $p<0.01$) (Table 3.1 and Fig. 3.8A).

The oceanic diatom, *T. oceanica,* did not exhibit significant differences in the cellular content of C, N, Si and P between Zn treatments (t-test, $p>0.01$) (Table 3.1, Fig. 3.8B). Although changes in elemental composition were not significant, N, Si and P content showed a 20% increasing trend under Zn limitation. For example, Si content per cell surface at Zn-limiting conditions was 0.87 ±0.07 fmol Si μm^{-2} (mean ± 1SE) compared to 0.69 ±0.003 fmol Si μm^{-2} (mean ± 1SE) at Zn-replete conditions. Carbon content exhibited a not significant decrease of 11% under Zn limitation (t-test, $p>0.01$).

Table 3.1 Cellular quotas of carbon (C), nitrogen (N), silicon (Si) and phosphorus (P) per cell, cell surface (only Si), and cell volume under Zn-replete and Zn-limiting conditions. Values represent the mean ± 1 SE of triplicate cultures.

Elemental quotas		*Skeletonema costatum*		*Thalassiosira oceanica*	
		Zn-replete	**Zn-limited**	**Zn-replete**	**Zn-limited**
C Quota	**pmol cell^{-1}**	6.26 ± 0.12*	2.32 ± 0.12*	2.96 ±0.17	2.94 ±0.14
	fmol µm^{-3}	15.05 ± 0.56*	22.85 ± 1.19*	24.18 ±0.44	21.45 ±1.06
N Quota	**pmol cell^{-1}**	0.77 ± 0.03*	0.26 ± 0.02*	0.20 ±0.02*	0.31 ±0.00*
	fmol µm^{-3}	2.20 ± 0.07	2.59 ± 0.17	1.91 ±0.15	2.32 ±0.03
Si Quota	**pmol cell^{-1}**	0.63 ± 0.02	0.15 ± 0.01	0.10 ±0.04	0.13 ± 0.01
	pmol µm^{-3}	1.63 ± 0.05	1.48 ± 0.10	0.78 ±0.02	0.96 ±0.07
	fmol µm^{-2}	2.36 ± 0.07*	1.19 ± 0.03*	0.69 ±0.00	0.87 ± 0.07
P Quota	**pmol cell^{-1}**	0.07±0.00*	0.03±0.00*	0.04 ±0.00	0.06 ±0.00
	fmol µm^{-3}	0.18 ± 0.01*	0.28 ± 0.01*	0.34 ±0.03	0.42 ±0.03

* Indicates significant change in elemental ratios between Zn-replete and Zn-limiting conditions (t-test, $p<0.01$).

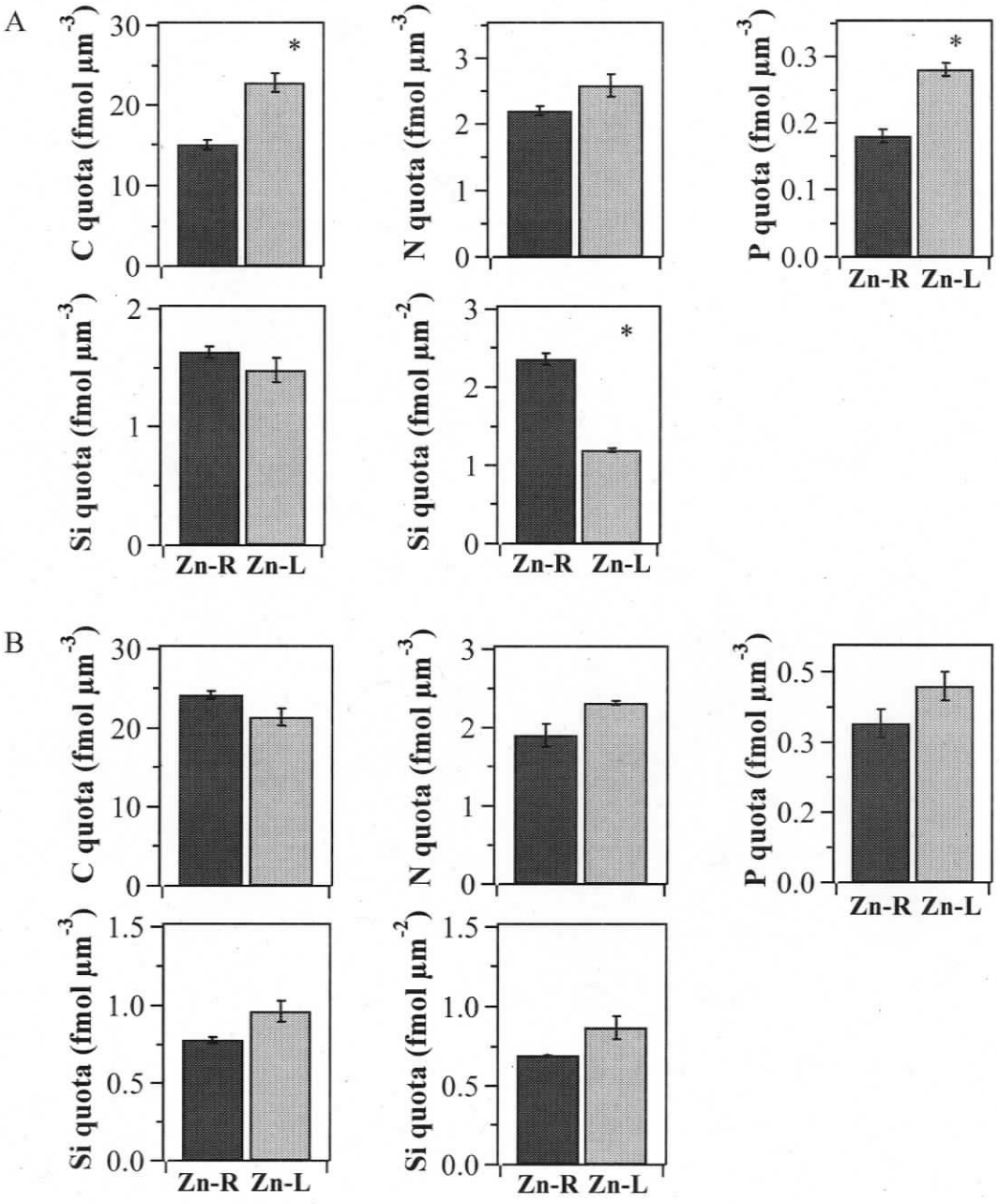

Fig. 3.8 Cellular quotas of carbon (C), nitrogen (N), silicon (Si) and phosphorus (P) per cell volume and surface (only Si) at Zn-replete (Zn-R) and Zn-limiting (Zn-L) conditions in *Skeletonema costatum* (A) and *Thalassiosira oceanica* (B). Bars represent the mean ± 1 SE of triplicate cultures (same data as in Table 3.1). * Indicates significant change in elemental quota between the two Zn treatments (t-test, $p<0.01$).

Elemental ratios:

Skeletonema costatum showed significant differences only for the following elemental ratios: $Si_s:C_v$ and $Si_s:N_v$, between Zn-replete and Zn-limiting conditions (t-test, $p<0.01$) (Table 3.2 and Fig. 3.9A) . The Si/C and Si/N ratios decreased under Zn limitation, but the magnitude of this decrease was less when the Si quota was normalized per cell volume than when it was normalized per cell surface. The ratio Si/C decreased by 38% ($Si_v:C_v$ from 0.11 to 0.07) or by 70% ($Si_s:C_v$ from 0.16 to 0.05) under Zn limitation. The Si/N ratio decreased in mean values from 28% ($Si_v:N_v$ from 0.76 to 0.55) to 60% ($Si_S:N_v$ from 1.10 to 0.44) under Zn-limiting conditions. Under Zn-replete conditions the $C_v:N_v$ ratio (6.85±0.19, mean ± 1SE) was in agreement with Redfield proportion (106C:16N = 6.62), and it was slightly higher at Zn limiting conditions. The $C_v:P_v$ and $N_v:P_v$ ratios did not exhibit significant differences, however the $N_v:P_v$ ratio decreased by 25% under Zn limitation (t-test, $p>0.01$). In summary, the elemental stoichiometry of the coastal diatom *S. costatum* was 82C : 9N : 5Si : 1P under Zn-limitation and 84C : 12N : 9Si : 1P under Zn-replenishment.

The oceanic diatom, *T. oceanica,* did not exhibit any significant differences in elemental ratios between Zn treatments (t-test, $p>0.01$) (Table 3.2 and Fig. 3.9B). However the $C_v:N_v$ and C_v:P ratios showed a decrease of 28% under Zn limitation. In addition, the $Si_s:N_v$ was between one half to three-quarters lower than the expected Si:N ratio of 1.05 (Brzezinski, 1985), regardless of the Zn nutritional condition. In summary, *T. oceanica* elemental stoichiometry was 51C : 6N : 2S : 1P under Zn-limitation and 71C : 6N : 2Si : 1P under Zn-replenishment.

Table 3.2 Elemental molar ratios normalized by cell number, cell surface (only Si) and cell volume under Zn-replete and Zn-limiting conditions. Values represent the mean ± 1 SE of triplicate cultures. Subscript symbols are c = cell; v = volume and s = surface area. Units are mol:mol.

Elemental Ratios		*Skeletonema costatum*		*Thalassiosira oceanica*	
		Zn-replete	Zn-limiting	Zn-replete	Zn-limiting
C:N	$C_C:N_C$	8.16±0.27	8.81±0.26	15.06±2.01	9.43 ±0.40
	$C_V:N_V$	6.85± 0.19	8.85±0.27	12.85±1.23	9.22 ±0.47
Si:C	$Si_V:C_V$	0.11±0.00	0.07±0.01	0.03±0.00	0.04±0.00
	$Si_S:C_V$	0.16±0.00*	0.05±0.00*	0.03±0.00	0.04±0.00
Si:N	$Si_V:N_V$	0.76± 0.02	0.55±0.07	0.38±0.01	0.39±0.04
	$Si_S:N_V$	1.10±0.02*	0.44±0.05*	0.34±0.00	0.36±0.04
C:P	$C_C:P_C$	84.67±5.57	81.16±2.19	65.72±2.05	51.86±5.94
	$C_V:P_V$	84.41±4.84	82.26±2.41	71.20±5.20	51.34±6.12
N:P	$N_C:P_C$	10.37±0.47	9.24±0.49	4.53±0.64	5.47±0.42
	$N_V:P_V$	12.31±0.36	9.32±0.54	5.57±0.26	5.53±0.34

* Indicates significant change in elemental ratios between Zn-replete and Zn-limiting conditions (t-test, $p<0.01$).

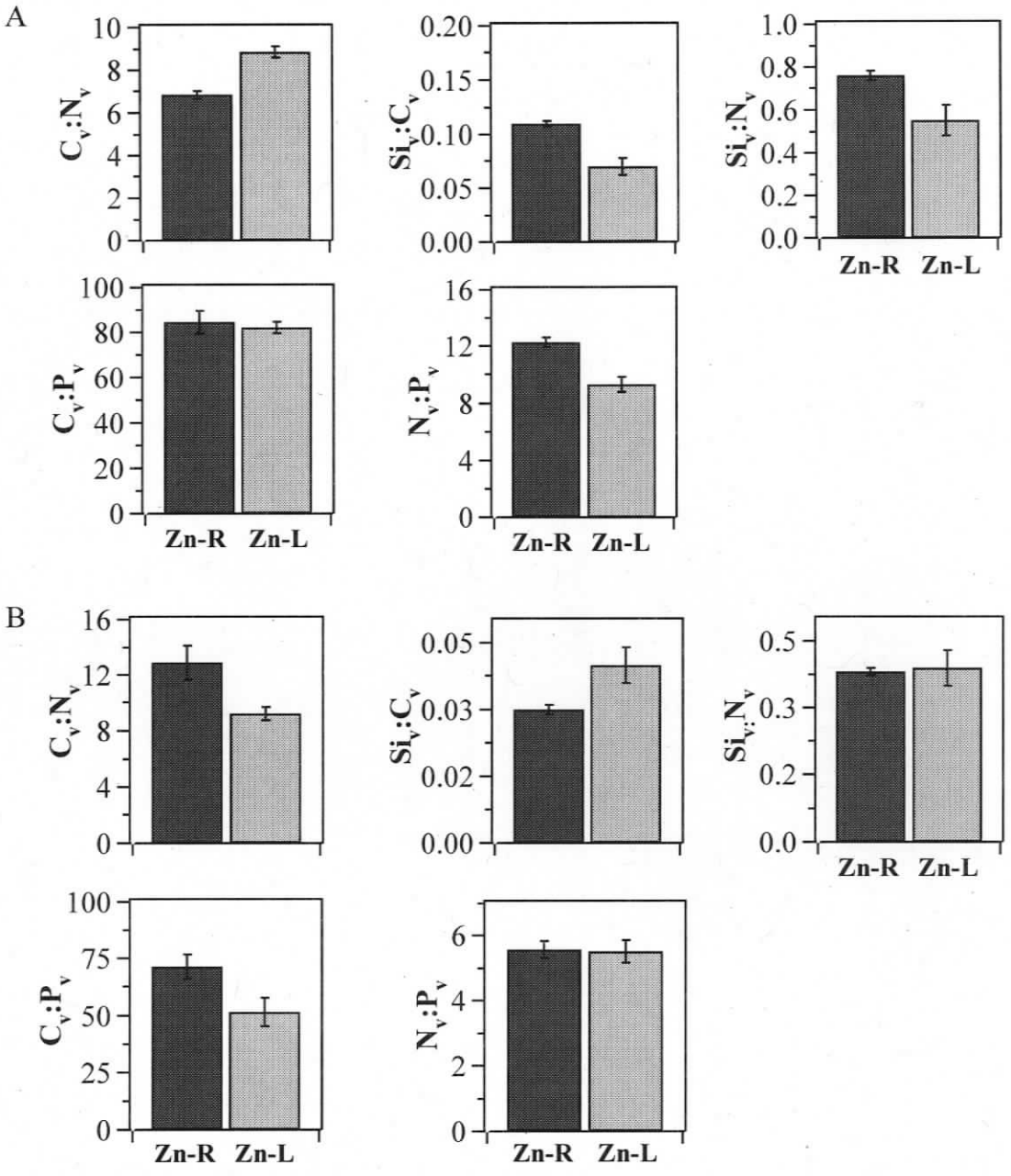

Fig. 3.9 Elemental molar ratios C:P, Si:C, Si:N, C:P and N:P at Zn-replete (Zn-R) and Zn-limiting (Zn-L) conditions in *Skeletonema costatum* (A) and *Thalassiosira oceanica* (B). Bars represent the mean ± 1 SE of triplicate cultures (same data as in Table 3.1). Units are mol:mol.

3.2.4 Incorporation of macronutrients at Zn-replete and Zn-limiting conditions

The coastal diatom *S. costatum* did not exhibit differences in the incorporation of C between Zn-replete conditions (12.06±0.64 fmol C μm^{-3} day^{-1}) and Zn-limiting conditions (12.65±0.98 fmol C μm^{-3} day^{-1}) (Fig. 3.10A). Yet, *T. oceanica* cultures showed a significant decrease in the incorporation of C from Zn-replete to Zn-limited cells. At Zn-limiting conditions, the incorporation rate of C in the oceanic diatom dropped significantly by 50% from 13.13±0.65 to 6.55.±1.22 fmol C μm^{-3} day^{-1} (mean±SE) (t-test, $p<0.01$). The N incorporation rate dropped by 30% (from 1.69±0.13 to 1.17.±0.10 fmol N μm^{-3} day^{-1}) in *S. costatum* and by 45% (from 1.63±0.22 to 0.90±0.12 fmol C μm^{-3} day^{-1}) in *T. oceanica* under Zn limitation; however these changes were not statistically significant (t-test) at $p>0.01$ (Fig. 3.10B). The P incorporation rate decreased, but also not significantly, by 45% (from 0.22±0.01 to 0.12.±0.00 fmol P μm^{-3} day^{-1}) in *S. costatum* and by 19% (from 0.22±0.08 to 0.18.±0.05 fmol P μm^{-3} day^{-1}) in *T. oceanica* under Zn limitation (t-test, $p>0.01$) (Fig. 3.10C).

Silicon incorporation rates were calculated per cell volume and cell surface (Fig. 3.11). In *S. costatum* the incorporation rate of Si per cell volume and cell surface significantly decreased under Zn limitation (t-test, $p<0.01$). Under Zn limitation, mean incorporation rates dropped by 62% (from 1.90±0.11 to 0.73±0.04 fmol Si μm^{-3} day^{-1}) or by 80% (from 2.81±0.13 to 0.61±0.00 fmol Si μm^{-2} day^{-1}). However, in *T. oceanica* the incorporation rate of Si (normalized per cell volume or surface) showed a not significant increase of ~30% (t-test, $p>0.01$)

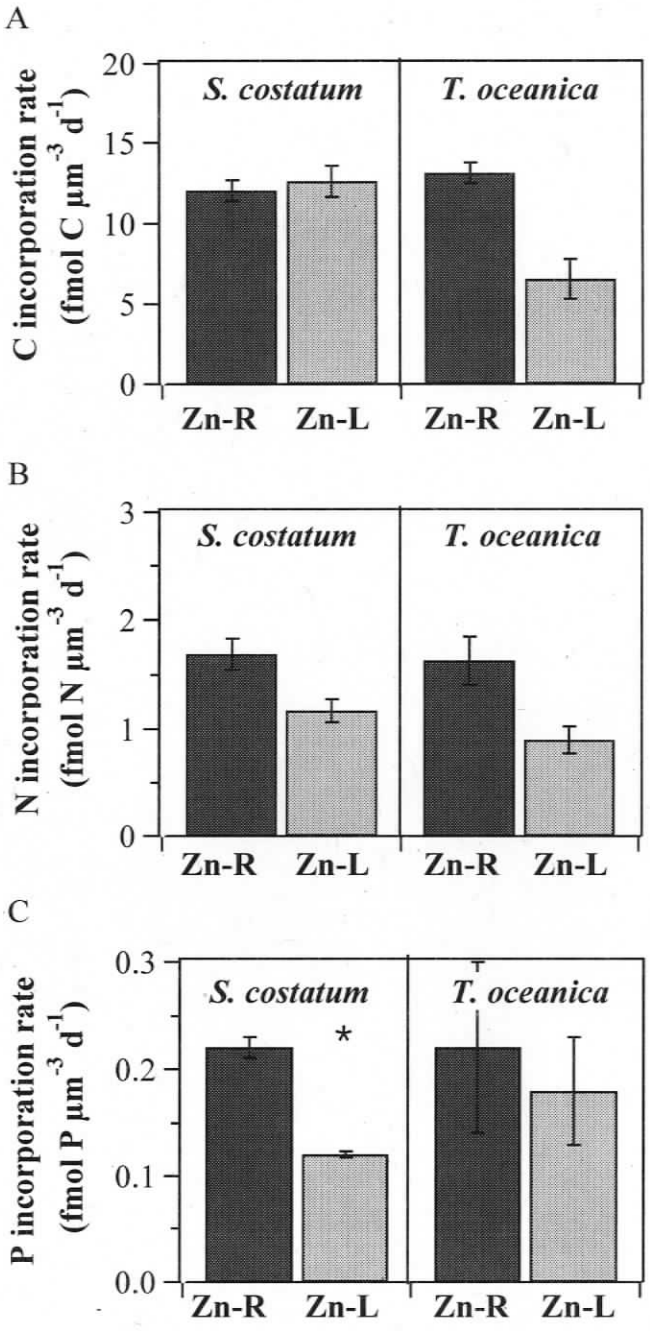

Fig. 3.10 Incorporation rates of carbon (A), nitrogen (B), and phosphorus (C) at Zn-replete (Zn–R) and Zn-limiting (Zn–L) conditions in *Skeletonema costatum* and *Thalassiosira oceanica*. Bars represent the mean ± 1 SE of triplicate cultures. * Indicates significant change in elemental quota between the two Zn treatments (t-test, $p<0.01$).

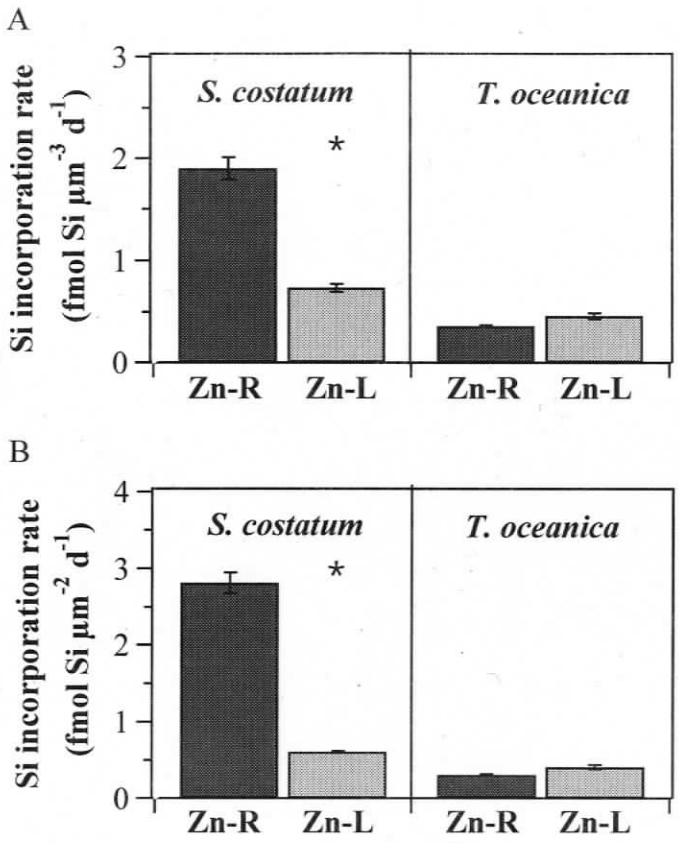

Fig. 3.11 Incorporation rate of biogenic silica (BSi) per cell volume (A) and per cell surface (B) at Zn-replete (Zn–R) and Zn-limiting (Zn–L) conditions in *Skeletonema costatum* and *Thalassiosira oceanica*. Bars represent the mean ± 1 SE of triplicate cultures. * Indicates significant change in elemental quota between the two Zn treatments (t-test, $p<0.01$).

3.2.5 Comparison between depletion of dissolved macronutrients in the culture media and incorporation of macronutrients into the cells

The rate of incorporation of macronutrients was calculated from the increase in elemental content in the cells (Section 3.2.4). To confirm that mass balance was achieved during these experiments, the depletion of dissolved NO_3^-, $Si(OH)_4$ and HPO_4^{2-} were compared to the increases in PON, BSi and POP in the culture media (Fig. 3.12). The regression coefficients between nutrient depletion and particulate content were r^2 = 0.95 for PON/ NO_3^-, r^2 = 0.98 for BSi/$Si(OH)_4$ and r^2 = 0.89 for POP/HPO_4^{2-}. The high regression coefficients confirm that there was mass balance in these culture experiments and support the calculation of incorporation rates from the elemental quotas.

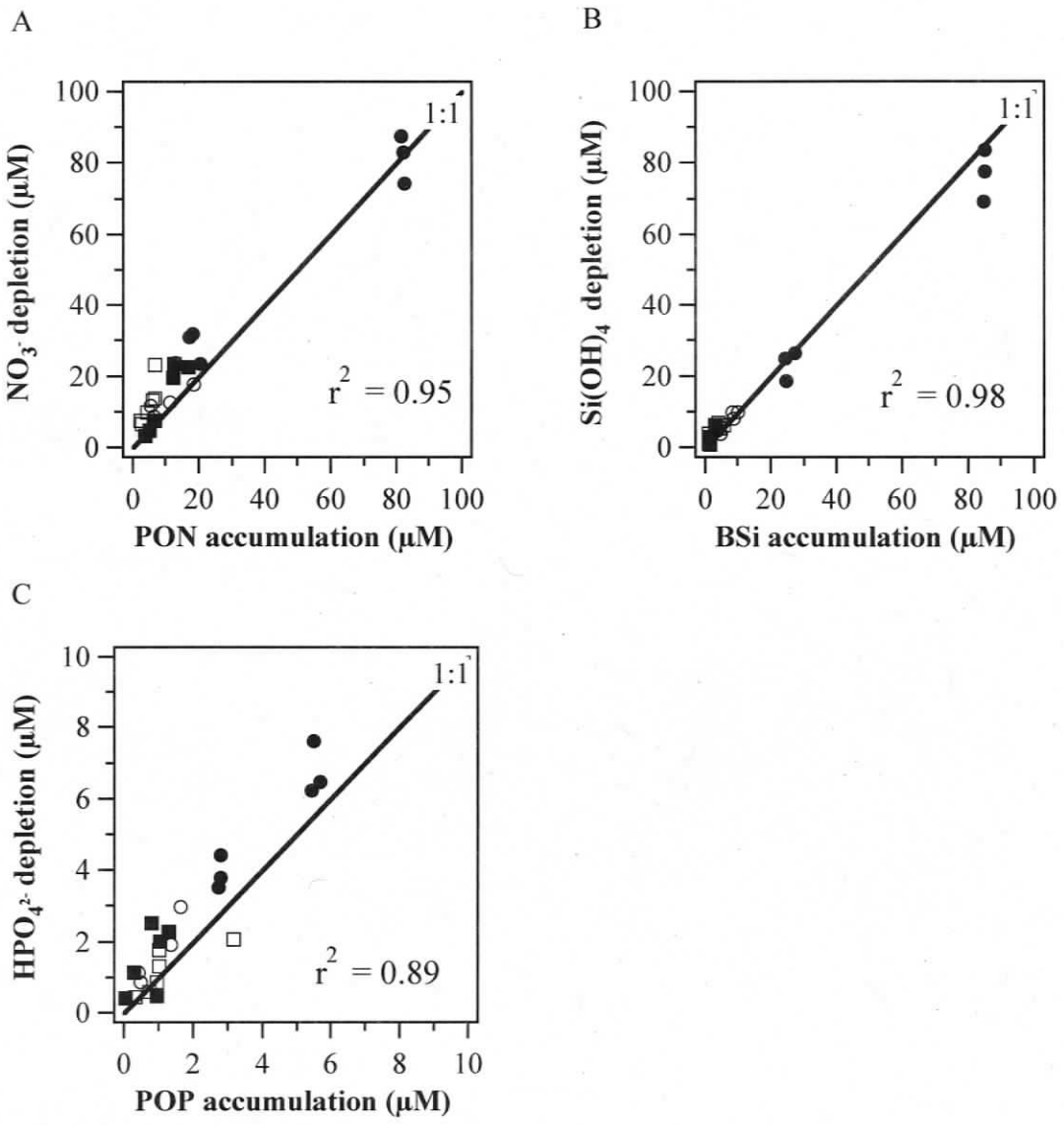

Fig. 3.12 Relationship between dissolved nutrient depletion from the culture media and incorporation of N, Si and P into particulate organic matter. (A) Depletion of NO_3^- vs. particulate organic nitrogen (PON) concentration, (B) depletion of $Si(OH)_4$ vs. biogenic Si (BSi) concentration, and (C) depletion of HPO_4^{2-} vs particulate organic phosphorus (POP) concentration. Symbols represent values for each culture in: (●) Zn-replete *Skeletonema costatum*; (○) Zn-limited *S. costatum*; (■) Zn-replete *Thalassiosira oceanica*; and (□) Zn-limited *T. oceanica*. The r^2 is the regression coefficient.

CHAPTER 4 – DISCUSSION AND CONCLUSIONS

DISCUSSION

This is the first study to report the effects of Zn limitation on the cellular quotas C, N, Si and P of an oceanic diatom. Furthermore, the elemental composition and the elemental ratios of a coastal diatom in steady state conditions have not been previously examined under Zn limitation, nor has been the interaction between Zn limitation and cell morphology. These results should provide new insights into the role of Zn on the distribution of diatom species, the composition of phytoplankton assemblages and nutrient cycling by diatoms in the oceans. The main results from these experiments are discussed below with special emphasis on the differences between the two diatoms and the ecological implications of observed phytoplankton response.

Effect of Zn availability on the growth rates of marine diatoms

In this study, the effect of Zn^{2+} availability on growth rates of *S. costatum* and *T. oceanica* were described with a Monod model. The μ_{max} estimated under optimal conditions was 1.44 d^{-1} for the coastal *S. costatum* and 0.92 d^{-1} for the oceanic *T. oceanica*. Previous studies with *S. costatum* reported maximum growth rates in the range of 1.45 to 2.88 d^{-1} under optimal growth conditions and at a similar experimental temperature (Eppley and Sloan, 1966; Davis et al., 1973). In the case of *T. oceanica,* most of the previous studies measured growth rates in the range of 1.0 to 1.5 d^{-1} (Sunda and Hunstman, 1992; Lee and Morel, 1995; Strezepek and Harrison, 2004). Thus, the maximum growth rates observed here fell within those previously found.

The estimated $K_{s\text{-}Zn}$ in our study was 10 times lower in the oceanic than in the coastal diatom (4.46 $x10^{-13}$ Zn^{2+} M for *T. oceanica* and 4.07 $x10^{-12}$ Zn^{2+} M for *S. costatum*). In addition, *S. costatum* exhibited a minimum Zn^{2+} concentration (2.64 $x10^{-12}$ ± 8.27 $x10^{-14}$ M), below which cells were unable to grow. The ability of the oceanic species to grow at lower Zn^{+2} concentrations than those required by coastal species is in agreement with previous studies (Brand et al., 1983; Sunda and Huntsman, 1992). Sunda and Hunstman (1995) showed that oceanic species could maintain maximum growth rates at low [Zn^{2+}] by reducing their internal Zn requirements. Furthermore, these studies concluded that differences in micronutrient requirements such as Fe and Zn were important in determining the geographical distribution and evolution of oceanic versus coastal phytoplankton species.

Effect of Zn availability on the cell morphology of marine diatoms

Diatoms have the ability to adapt to environmental stress by altering their cell morphology. In this study, low Zn availability significantly affected the cell size parameters (i.e., surface area and volume) in the coastal diatom *S. costatum*, but did not have any influence on the oceanic diatom *T. oceanica*. Under the lowest Zn concentrations, cells of *S. costatum* reduced their cell volume twice as much as they reduced their cell surface, and thus, their S/V ratio increased by 80% from the S/V ratio characteristic of Zn-replete cells. Previous studies have also measured a decrease in cell volume and an increase in S/V ratio under limitation by Fe (Leynaert et al., 2004; Marchetti and Harrison, 2007) and macronutrients (Harrison et al., 1977; Lynn et al., 2000). This increase in S/V ratio likely occurs to maximize nutrient uptake and diffusion at low ambient Zn concentrations.

Nutrient requirements are mainly related to cell volume whereas uptake rates are mainly associated with the amount of cellular surface exposed to the environment. Thus, an increase in the S/V ratio would maximize the transport of nutrients across the cell membrane. Cells with greater S/V ratio would experience increased exchanges of gases and solutes across the cell surface, which decrease the diffusion limitation of nutrient uptake in comparison to cells with lower S/V ratios (Morel et al., 1991). Therefore, *S. costatum* morphological changes resulted in an increased S/V ratio, which is an important strategy for adaptation to micronutrient stress.

The changes in cell morphology in *S. costatum* can be analyzed with the model of Pahlow et al. (1997), which describes the effects of cell shape and chain length on nutrient acquisition by diatoms. The model assumes that cell shape can influence nutrient supply to the cell surface either by affecting diffusion or by changing advective transport. According to the model, elongated cells have a greater surface area than spherical cells of the same volume and the reduction in solute diffusion due to chain formation is less pronounced if the chain consists of elongated cells (Pahlow et al., 1997). Thus, narrow and elongated cells in the chain-forming *S. costatum* (see Fig. 3.3) would enjoy greater diffusion and have larger S/V ratios, and therefore this morphology would be more favourable under Zn limitation. In contrast, longer and thicker chains would have greater advective transport, but this cannot compensate for the reduction in diffusive transport per unit of surface area (Pahlow et al., 1997). This may explain why fewer cells per chain were observed in Zn limited cultures in contrast to Zn-replete cultures during this study.

In the case of *T. oceanica,* the cell morphology was unaffected by Zn availability. However, according to the studies of Sunda and Hunstman (1992, 1995), Zn uptake rates

of *T. oceanica* approach diffusion limitation to the cell surface at $[Zn^{2+}]$ lower than 1 pmol L^{-1}. Yet, the already small cell dimension of this species together with a round shape could limit the ability to increase the cell surface area in relation to cell volume. In addition, *T. oceanica* was isolated from an oligotrophic ocean (Sargasso Sea), and it might have already evolved to maximize its cell morphology to succeed in low nutrient environments.

The ability of diatoms to alter their cell morphology represents an important adaptation to nutrient stress and emphasizes the plasticity of this group under a changing environment. Cell shape plasticity has probably played an important role in the evolution of cell forms and colonization of new environments by diatoms.

Effect of Zn nutritional status on the chlorophyll *a* quota of marine diatoms

The Chl-*a* quotas measured in *S. costatum* and *T. oceanica* in this study agreed with the findings of Sunda and Huntsman (1995) in that a reduction (15-20%) of Chl-*a* was observed under Zn-limiting conditions. Furthermore, as reported here for *S. costatum*, a decrease in the Chl-*a*:C ratio under Zn-limiting conditions was previously observed in *T. pseudonana* (Sunda and Huntsman, 2005). Several other studies have also reported decreases in the Chl-*a*:C ratio under nutrient stress (e.g. $Si(OH)_4$, N, Fe) in diatoms. However, in this study Zn limitation did not have any effect on the Chl-*a*:C ratio of *T. oceanica*.

Since there is no evidence that Zn is involved in the synthesis of Chl-*a*, this reduction in pigment content (i.e. chlorosis) may be an indirect effect of Zn limitation due to a decrease in growth rates. Lower growth rate under Zn limitation might result in lower

energy requirement by the cell, and consequently in a reduction of the light harvesting system. In addition, the decrease in Chl-*a* can be the result of a reduction in the C fixation rate due to a decrease in the activity of CA. Moreover, given that the intracellular concentration of Chl-*a* tends to decrease with cell size (Finkel, 2001), this could also be a factor responsible for the decrease in Chl-*a* in *S. costatum*.

Effect of Zn nutritional status on the elemental composition, incorporation rates and elemental ratios in marine diatoms

Zinc limitation resulted in a significant increase in C quotas only in the coastal diatom. This result agrees with the single published study that investigated the effects of Zn limitation on elemental quotas of a marine diatom (*T. weissflogii*) (De La Rocha et al., 2000). De La Rocha et al. (2000) reported a 55% increase in C content per cell at Zn-limiting conditions. Changes in C content of marine diatoms due to limitation by micronutrients have been studied more extensively for Fe. However, there is no agreement in the literature regarding the effects of Fe limitation on C content. Previous studies indicated no change (Price, 2005), an increase (Muggli and Harrison, 1996; De La Rocha et al., 2000) or a decrease (Maldonado and Price, 1996; Marchetti and Harrison, 2007) in C quotas under Fe limitation. Iron effects on C content are explained by the essential role of Fe in C assimilation pathways and energy acquisition. In the present study, changes in C content of *S. costatum* could be associated to an increase in storage pools (carbohydrates and lipids) under Zn-limiting conditions, since C incorporation rates did not change with Zn condition.

Nitrogen content did not exhibit any changes between Zn-replete and Zn-limited cells of *S. costatum* and *T. oceanica*. The study of De La Rocha et al. (2000) cite an increase in N content with Zn limitation, but differences between this study and our results could have arisen from a different normalization of the elemental quotas (i.e, per cell in *T. weissflogii* and per cell volume in *S. costatum* and *T. oceanica*). In De La Rocha et al. (2000), the increase of N (and C) content was attributed to a delay in cell division under Zn limitation, which may allow for a greater accumulation of cellular materials in Zn-limited compare to Zn-replete cells. As it is the case for C content, there is no agreement among studies about the effect of Fe limitation on N quotas (Maldonado and Price, 1996; Marchetti and Harrison, 2007; Muggli and Harrison, 1996; De La Rocha et al., 2000). However, despite the different responses reported by these studies, Fe and Zn limitation resulted in the same direction of change for both nutrients (C and N). In contrast, the present study showed different tends in C and N content of *S. costatum* under Zn limitation, indicating that C and N metabolisms may not always be tightly coupled.

Zn availability affected Si content in opposite directions in the coastal and the oceanic diatom. In *S. costatum,* Si content decreased, whereas in *T. oceanica*, Si content increased (although not significantly) under Zn limitation. The other single study that investigated the effects of Zn limitation on elemental quotas reported an increase (55%) of Si content per cell at Zn-limiting conditions in *T. weissflogii* (De La Rocha et al., 2000). However, comparison with the later study is limited due to a different normalization of Si content. In addition, the observed reduction of cell size in *S. costatum* with Zn limitation emphasize the significance of normalizing elemental quotas per unit of

surface area or per unit of volume. As for Si, cells growing at exponential phase have low internal pools, and Si is associated with the frustule (Thamatrakoln and Hildebrand, 2008), which suggests that cellular Si should be expressed as Si per unit of surface area.

In regards to effects of other metals on Si content, coastal and oceanic *Pseudo-nitzschia* sp. exhibited a slight decrease (although not uniform among isolates) in Si per cell surface under Fe limitation (Marchetti and Harrison, 2007). But most studies showed an increase of Si content under Fe-limited conditions (Takeda, 1998; De La Rocha et al., 2000; Hutchins and Bruland, 1998; Leynaert et al., 2004). Increase of Si under micronutrient limitation was attributed to the link between silica deposition and the duration of the cell cycle (Martin-Jezequel et al., 2000). An increase in the length of the cell cycle under low growth conditions allows maximum incorporation of Si into the frustule (Martin-Jezequel et al., 2000). However, this does not explain the results of this study and the decrease of Si in the coastal diatom *S. costatum* suggests an additional effect of Zn on Si metabolism.

Rueter and Morel (1981) were the first to suggest that Zn could be involved in $Si(OH)_4$ uptake in *T. pseudonana*. The study of the De La Rocha et al. (2000) found that the affinity of the Si transport system was Zn-dependent in *T. weissflogii*, indicating that Zn was required for BSi production. In the present study, *S. costatum* exhibited up to an 80% reduction of Si incorporation rates under Zn limitation, indicating also a role of Zn in Si metabolisms. Sherbakova et al. (2005) suggested that a conserved Motif CMLD could acts as a Zn-binding site, and that this structure could be directly involved in transporting $Si(OH)_4$. These findings support the hypothesis that Zn is required for Si

metabolisms in marine diatoms, and thus Zn limitation would decrease $Si(OH)_4$ uptake and biogenic silica production. In addition, unlike C, N and P, Si incorporations rates at Zn-replete conditions exhibited lower values in *T. oceanica* (0.31±0.01 fmol Si μm^{-2} day^{-1}) compared to *S. costatum* (2.81±0.13 fmol Si μm^{-2} day^{-1}), which could be explained by a less silicified cell in the oceanic diatom (see Fig. 3.11 and Table 3.1).

This is the first study to assess the effect of Zn limitation on the P content of marine diatoms. According to Price (2005), excess consumption of P is common at high HPO_4^{2-} concentrations and when other resources are limiting phytoplankton growth. Both diatom species in this study exhibited an increase in P content (although it was only significant for the coastal diatom). In addition, Ellwood and Hunter (2000) found that the uptake rate of P decreases less than that of Si under Zn limitation. Thus, luxurious consumption of P may also be the case when Zn is the limiting resource.

Despite the fact that CA activity was not measured during this study, the body of literature indicates a decrease in CA activity at low Zn concentrations (Morel et al, 1994; Lane and Morel, 2000; Morel et al., 2002; Sunda and Huntsman, 2005). Decrease in CA activity could lead to a decrease in the CO_2 available for the enzyme RUBISCO, and therefore the photosynthetic rate may be limited by C. In addition, Sunda and Huntsman (2005), reported that under severe Zn limitation, the relationship between specific growth rate and the cell Zn:C ratio decreased sharply and was not affected by changes in CO_2 availability in the coastal diatom *T. pseudonana*. They concluded, that under severe Zn limitation the biochemical demand for Zn was unlikely to be primarily linked to CA, but rather to other Zn proteins such as those involved in DNA replication and transcription. Therefore, a decrease in the amount of Zn finger proteins under Zn limitation could have

delayed DNA replication and transcription in the cell. Considering the findings of Sunda and Huntsman (2005) and the reduction in growth rates measured in the present study (~40% μ_m in both species), then the observed changes in the elemental composition of *S. costatum* and *T. oceanica* could have been driven by a decrease of Zn finger proteins.

Variability in the ratios of the main elements (C, N, Si and P) are indicative of a differential effect of Zn limitation on their metabolisms. Zinc limitation mainly affected the elemental stoichiometry of the coastal diatom *S. costatum* by decreasing the Si:C and Si:N ratios. De La Rocha et al. (2000) observed an increase of Si:C and Si:N ratios of *T. weissflogii* under Zn limitation. The differences between the later study and the results of this project result from the opposite trends in Si content under Zn limitation. However, the identification of the physiological reasons behind these variations needs further research.

The elemental stoichiometry of coastal diatom *S. costatum* was 84C : 12N : 9Si : 1P under Zn-replenishment and 82C : 9N : 5Si : 1P under Zn-limitation, indicating a relative decrease in the proportion of Si. In comparison, the elemental stoichiometry of the oceanic diatom *T. oceanica* was 71C : 6N : 2Si : 1P under Zn-replenishment and 51C : 6N : 2Si : 1P under Zn-limiting, indicating a relative decrease in the proportion of C. Although Zn-limited cells may be able to carry out luxury consumption of P and hence increase the storage pools of P (e.g. inorganic polyphosphate), significant changes in Si incorporation by *S. costatum* and C incorporation by *T. oceanica* suggest other effects of Zn availability on the metabolisms of these two elements, which are not elucidated to date.

Ecological implications

The extent of Zn limitation on phytoplankton production in today's oceans is not fully assessed, but it has been suggested that it is more likely to occur in coastal environments or during phytoplankton blooms (Brand et al., 1983; Coale et al., 1991; Franck et al., 2003; Crawford et al., 2003; Sunda and Hundtsman, 2005). In addition, Zn demands increase at low CO_2 concentration, which often occurs during algal blooms in eutrophic coastal waters (Morel et al. 1994; Sunda and Hunstman, 2005). It is also during these conditions that diatoms are the predominant group in phytoplankton communities. Overall, our laboratory results support the hypothesis that Zn availability would mainly affect the cellular morphology and physiology of diatoms inhabiting coastal environments.

Based on the findings of this study, it is unlikely that Zn would significantly affect Redfield ratios in open oceans. *T. oceanica* which has been chosen as a representative of oceanic species, appears to be physiologically adapted to Zn concentration commonly found in oceanic waters. However, in coastal environments Zn availability could affect the Si:C and the Si:N ratio of phytoplankton cells. In addition, changes in C content of coastal phytoplankton species under Zn limitation could affect the biological pump since recent studies have stressed the importance of coastal margins in carbon export to deep waters (Muller-Karger et al., 2005; Hales et al., 2006). Based on the effect of Zn availability on the coastal diatom *S. costatum*, it is more likely that Zn would have a stronger effect on the efficiency of the biological pump in coastal environments rather than in oceanic waters.

CONCLUSIONS

This thesis provides new information on the effects of Zn availability on growth rate, cell morphology and nutrient physiology in diatoms from two contrasting marine environments. The main finding of this thesis were:

- The coastal diatom *Skeletonema costatum* had a higher Zn^{2+} requirement for growth than the oceanic diatom *Thalassiosira oceanica.*
  - *S. costatum* did not grow at $[Zn^{2+}]$ lower than $2.64 \times 10^{-12} \pm 8.27 \times 10^{-14}$ M, and the estimated $K_{s\text{-}Zn}$ for growth was $4.07 \times 10^{-12} \pm 4.15 \times 10^{-13}$ M.
  - *T. oceanica* grew at all tested $[Zn^{2+}]$, and the estimated $K_{s\text{-}Zn}$ for growth was $4.46 \times 10^{-13} \pm 9.65 \times 10^{-14}$ M.
- Zn availability had significant effects on the cell morphology of the coastal diatom, but it did not affect the cell morphology of the oceanic diatom.
  - *Skeletonema costatum* increased the cell S/V ratio under Zn-limiting conditions to favor a higher diffusion rate and uptake area.
- Chlorophyll *a* content slightly decreased at limiting $[Zn^{2+}]$ in both species, but differences were significant only for *S. costatum.*
- The Chl-a:C ratio decreased at limiting $[Zn^{2+}]$ in *S. costatum,* but did not show differences in *T. oceanica* between Zn conditions.
- Under limiting $[Zn^{2+}]$, *S. costatum* exhibited the following significant changes in elemental composition, elemental ratios and incorporation rates:
  - An increase in the cellular quota of C and P, and a decrease in Si quota.

- A decrease in the elemental Si:C and Si:N ratios.
- A decrease in Si incorporation rates.

- The elemental stoichiometry of the coastal diatom *S. costatum* was 82C : 9N : 5Si : 1P under Zn-limitation and 84C : 12N : 9Si : 1P under Zn-replenishment.
- Under limiting $[Zn^{2+}]$, *T. oceanica* did not exhibit significant changes in the cellular quotas of C, N, Si and P, or in elemental ratios.
- Under limiting Zn^{2+} concentrations, *T. oceanica* exhibited a significant decrease in C incorporation rates.
- The elemental stoichiometry of the oceanic diatom *T. oceanica* was 51C : 6N : 2Si : 1P under Zn-limitation and 71C : 6N : 2Si : 1P under Zn-replenishment.

In summary, Zn limitation mainly affected the growth, cell morphology, nutrient uptake ratios, elemental composition and ratios in the coastal diatom *S. costatum*. The oceanic diatom *T. oceanica* seems to be physiologically adapted to low Zn environments. Therefore, Zn availability in the oceans is more likely to have an effect on phytoplankton in coastal environments.

FUTURE RESEARCH

The study of phytoplankton physiology and the interaction between the availability of trace metals and macronutrient physiology will provide us with a better understanding of the factors that control primary production and carbon export in the oceans. The results from this and previous studies on the effects of Zn on diatom physiology highlight new research directions that require further attention, such as:

1. Determination of the kinetic parameters (V_{max} and K_s) of macronutrient uptake in different diatom species under Zn limitation. This will allow us to explain and predict species dominance in natural phytoplankton assemblages. For example, the species with the lowest K_s values under Zn limitation will have a competitive advantage at low macronutrient concentrations, and may dominate the phytoplankton community.

2. Study of the relationship between Zn availability and silicic acid uptake kinetics. This will allow us to determine if Zn is a required element for silicic acid uptake in marine diatoms, as suggested by Rueter and Morel (1981).

3. Determination of the cell composition in terms of carbohydrates, phospholipids, proteins, amino acid, Zn content along with the activities of enzyme in which Zn is involved. Coupled elemental analysis of major macromolecules will give us insights into the effects of Zn limitation at the cellular level.

4. Determination of the response of acclimated cells and non-steady state cells to Zn limitation. Acclimated cells and non-steady cells could respond differently to Zn limitation with differential effects in cell composition and elemental stoichiometry. Results from experiments that address this question can be extrapolated to natural phytoplankton assemblages exposed to sudden limitation (e.g. after a blooming event) vs. chronic limitation.

5. Study of the effects of metal stress (e.g. Fe and Zn) on cell size of other ecologically relevant phytoplankton species, especially pennate diatoms. Changes in cell size and elemental quotas of marine diatoms due to metal stress can affect nutrient dynamics and carbon export in marine ecosystems.

APPENDIX A: TRACE METAL CLEAN TECHNIQUES

The following procedures were performed under trace-metal clean conditions:

(A) Cleaning of plasticware

(B) Preparation of Aquil media

(C) Manipulation of maintenance and experimental cultures

A) PROTOCOL FOR TRACE METAL CLEANING PLASTICWARE

The following procedures were performed to clean all plastic material used in culture work. Plasticware were:

1. Soaked in lab detergent Sparkleen® for at least 24 h
2. Rinsed with distilled water (DI) (5 or 6 times)
3. Rinsed with Milli-Q water (3 or 4 times). Milli-Q water is deionised water with a resistivity greater than 18.2 ΩM cm and dispensed by a Milli-Q system (Millipore Corporation).
4. Soaked in HCl 25% for at least 48 hours
5. Rinsed 3 times with Milli-Q water.

B) PROTOCOL FOR PREPARATION OF AQUIL MEDIA

Aquil medium was prepared following the procedures described by Price et al. (1988/1989) and Sunda et al. (2005). In summary, a Chelex 100 resin was used to remove metal contaminants present in ACS (American Chemical Society) reagent grade solutions of salts and nutrients. All metals were subsequently added back to the Aquil medium in an EDTA-buffered solution that controls their speciation and, thus, their availability to phytoplankton. In this study, natural seawater collected at Station PAPA (P or OSP; at 50°N latitude; 145°W longitude) in the HNLC Northeastern Pacific was used instead of

synthetic ocean water (prepared from reagent salts). In more detail, the following procedures were followed:

Part 1 - Purification of Chelex 100 and chelexing of natural seawater with added macronutrients:

These steps were followed to purify the Chelex 100 resin. Resin was:

6. Soaked in methanol for 3-4 h at room temperature (w/v = 40 g to 200 mL; rinsed with 2 L Milli-Q-H_2O). A scintered glass filter funnel was used in all rinsing steps.
7. Soaked in 1 M HCl at room temperature for 24 h. After 24 h, the resin was rinsed with Milli-Q-H_2O (~2 L).
8. Soaked in 3 M NH_4OH at room temperature for 1 week. Subsequently, the resin was rinsed with Milli-Q-H_2O (~2 L).
9. Soaked in 0.1 M HCl for 10 min, and rinsed with Milli-Q-H_2O (~2 L).
10. Rinsed with 200 ml of medium solution (Station PAPA seawater with added macronutrients).
11. Resuspended in 200 mL of medium solution and titrated slowly to pH 8.1 with 1M NaOH. This step usually took over a week.
12. Rinsed with medium and transferred to a polypropylene chromatography column.
13. Chelex 100 resin was now ready to use.

Natural seawater with added macronutrients was passed through a chromatography column packet with purified Chelex 100 resin. For each new batch of purified Chelex 100, the first 2 L of seawater were discarded before collecting media for culture work. All steps were done in a polypropylene Vertical Laminar Flow Clean Bench (Microzone Corporation).

Part 2 - Preparation of Media

Aquil medium was prepared with chelexed natural seawater from Station PAPA with added macronutrients. Concentrations of major nutrients, metals and vitamins in the medium are listed below:

Macronutrients

- $NaH_2PO_4 \cdot H_2O$ 1.00×10^{-5} M
- $NaNO_3$ 1.00×10^{-4} M
- $Na_2SiO_3 \cdot 9H_20$ 1.00×10^{-4} M

Metals

The stock metal solutions were prepared in 0.01 M HCl (Seastar®). The Fe stock solution was prepared and stored in 0.1 M HCl to avoid Fe precipitation. To prepare the EDTA-trace metals stock solution, each metal was added in appropriate concentrations from individual primary stocks to a 100 mM EDTA solution. Iron was added first and then the remaining trace metals.

- EDTA (anhydrous) 1.00×10^{-5} M
- $FeCl_3 \cdot 6H_2O$ 1.00×10^{-6} M
- $ZnSO_4 \cdot 7H_2O$ Various concentrations (see Chapter 2)
- $MnCl_2 \cdot 4H_2O$ 1.21×10^{-7} M
- $Na_2MoO_4 \cdot 2H_2O$ 1.00×10^{-7} M
- $CuSO_4 \cdot 5H_2O$ 1.96×10^{-8} M
- Na_2SeO_3 1.00×10^{-8} M

Vitamins

- Thiamine HCl (vitamin B) 2.97×10^{-7} M
- Biotin (vitamin H) 2.25×10^{-9} M
- Cyanocobalamin (vitamin B_{12}) 3.70×10^{-10} M

Part 3 - Sterilization of Media and Plastic materials

Microwave sterilization was utilized at every step of this study. This type of sterilization technique avoids contamination of the medium with metals. The protocol outlined by Keller et al. (1988) was followed to sterilize chelexed seawater with added nutrients. Filter-sterilized stock metal solutions, and Zn and vitamin solutions were added after microwave sterilization of the base medium using sterile techniques in a polypropylene Vertical Laminar Flow Clean Bench.

Microwave sterilization:

1. A 2L Teflon® bottle was filled with 1.5 L chelexed seawater with added macronutrients in the Clean Bench.
2. Microwave was wiped with 70% ethanol.
3. The bottle was put into the microwave with lid tightly closed.
4. Power was set at ≈ 700 W for 3 minutes.
5. Bottle was removed from microwave into the Clean Bench
6. Bottle was shaken and lid was momentarily opened to release pressure.
7. Steps 3 to 5 were repeated until seawater with added macronutrients started to boil.
8. Sterilize chelexed seawater with added macronutrients was allowed to cold down in the Clean Bench.

Plastic materials, e.g. medium bottles, were microwave sterilized following these steps:

1. Microwave was wiped with 70% ethanol.
2. Plasticware used for cultures (2L PC Bottles and 28 ml PC tubes) and pipette tips in plastic containers were filled with Milli-Q water.
3. Material was placed in microwave and power set at ≈ 700 W for enough time to allow water to boil.
4. Material was allowed to cold down in the Clean Bench

C) MANIPULATION OF CULTURES

The following precautions were taken to reduce metal contamination (Rueter and Morel, 1981):

1. Acid-clean treatment of all laboratory material.
2. Sterilization of media by microwave.
3. Transfer of cultures and media in the polypropylene Vertical Laminar Flow Clean Bench.
4. Wrapping of culture flasks with plastic bags.
5. Opening of culture flasks only in the Clean Bench.
6. No exposure of any part of the laboratory material to autoclave or flame.
7. Media and reagents kept in the TMC enclosure that consisted of a plastic tent with positive pressure provided by a plastic Air Cleaner with HEPA filter of plastic construction.

APPENDIX B: EFFECT OF IRRADIANCE ON GROWTH RATES OF *SKELETONEMA COSTATUM* AND *THALASSIOSIRA OCEANICA*

Introduction

Photosynthetically active radiation (PAR) modulates phytoplankton growth and elemental stoichiometry (Finkel et al., 2006). To study the effects of Zn availability on phytoplankton growth rates and nutrient physiology, it was essential to run experiments at optimal (and constant) light conditions.

The objective of these experiments was to determine the irradiance level at which *Skeletonema costatum* and *Thalassiosira oceanica* achieved maximum growth rates, i.e. optimum irradiance used for the Zn experiments.

Methods

Triplicate cultures of *S. costatum* and *T. oceanica* were grown at 20°C using a light: dark cycle of 14:10 h. *S. costatum* was exposed to six irradiance levels: 18, 60, 100, 130, 210 and 350 µmol photons m^{-2} s^{-1}. *T. oceanica* was exposed at five irradiance levels: 29, 111, 240, 306 and 500 µmol photons m^{-2} s^{-1}. Diatoms were grown in Aquil media (see Chapter 2 and Appendix A), but trace metal clean techniques were not required for these experiments.

Results and discussion

S. costatum reached maximum growth rates at irradiance levels between 210 to 350 µmol photons m^{-2} s^{-1}. The specific maximum growth rate was 1.18 ±0.03 d^{-1} (mean ±1 SE) (Fig. B.1).

For *T. oceanica,* maximum growth rates were achieved at irradiance levels between 240 to 500 µmol photons m^{-2} s^{-1}. The specific maximum growth rate was 0.80 ±0.03 d^{-1} (mean ± 1SE) (Fig. B.2.).

Thus, optimum irradiance level of 200 µmol photons m^{-2} s^{-1} and 240 µmol photons s^{-1} m^{-2} were utilized for the experiments done in this thesis with *S. costatum* and *T. oceanica*, respectively.

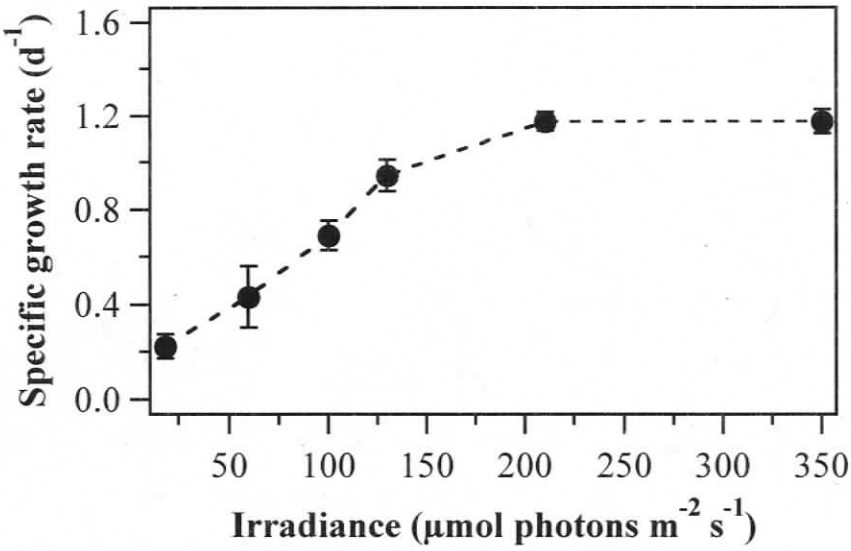

Figure B.1 Specific growth rates (µ) at different irradiance levels in *Skeletonema costatum*. Symbols represent the mean ± 1SE of triplicate cultures. When error bars are not visible, they are smaller than the symbol.

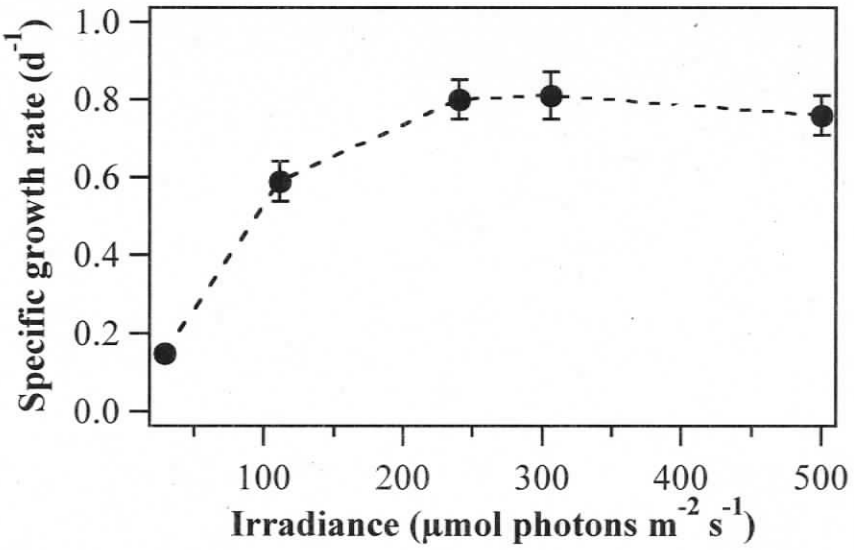

Figure B.2 Specific growth rates (µ) at different irradiance levels in *Thalassiosira oceanica*. Symbols represent the mean ± 1SE of triplicate cultures. When error bars are not visible, they are smaller than the symbol.

APPENDIX C: EFFECT OF COBALT ADDITIONS ON MAXIMUM GROWTH RATES IN *SKELETONEMA COSTATUM* AND *THALASSIOSIRA OCEANICA*

Introduction

Zinc (Zn) is an essential micronutrient for phytoplankton and a critical component of enzymes such as carbonic anhydrase (CA). In marine diatoms, Zn can be replaced by Cobalt (Co) or Cadmium (Cd) (Sunda and Huntsman, 1992; Morel et al., 2002). In addition, Co is normally added to Aquil medium due to a unique requirement in vitamin B_{12} (Sunda et al., 2005). However, Zn-limited and Zn-replete experiments were carried out without Co addition to avoid a potential Co interference and misinterpretation of the results from the Zn-limitation treatment.

The following experiment was carried out to test the effect of Co availability on the growth rates of *Skeletonema costatum* and *Thalassiosira oceanica*. The objective of this experiment was to confirm that Co was not an essential requirement for the growth of *S. costatum* and *T. oceanica,* and that eliminating Co from the media was not going to affect the growth rates of the diatoms.

Methods

Triplicate cultures of *S. costatum* and *T. oceanica* were grown at 20°C using a light: dark cycle of 14:10 h. Photosynthetically active radiation (PAR) was 200 µmol photons m^{-2} s^{-1} for *Skeletonema* sp. and at 240 µmol photons m^{-2} s^{-1} for *T. oceanica* (see Appendix B). Each species was grown in Aquil media with 7.97 x 10^{-8} M Zn added and

exposed to two treatments; no Co and 5.03 x 10^{-8} M Co. Cultures were grown using TMC techniques (see Chapter II and Appendix A).

Results and discussion

Specific maximum growth rates with or without Co were not significantly different in *S. costatum* or in *T. oceanica* (t-test, $p<0.01$) (Fig. C.1). These results confirmed that the elimination of Co does not have a deleterious effect on the growth rates of these species. Therefore, the Zn-replete and Zn-limiting experiments were carried out in this thesis without Co addition.

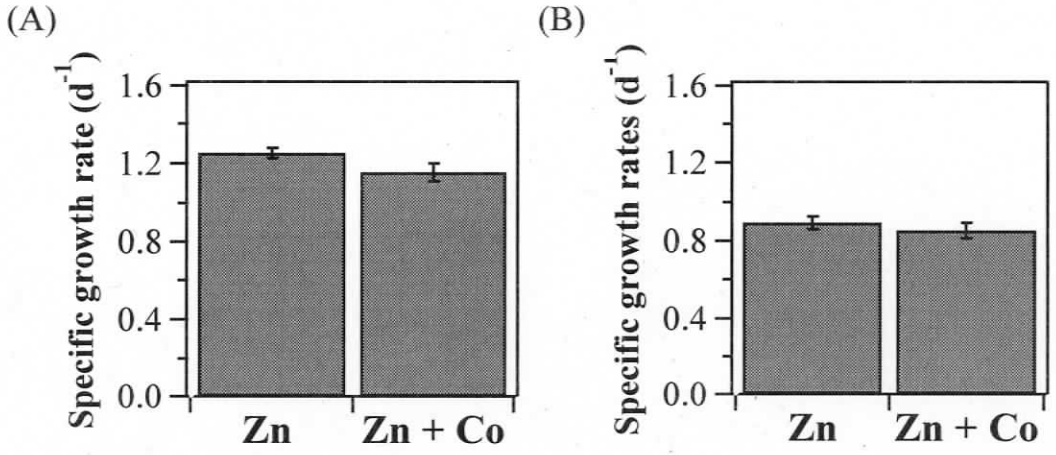

Figure C.1 Specific growth rates (μ) with zinc (Zn) and with zinc + cobalt (Zn+Co) in *Skeletonema costatum* (A) and *Thalassiosira oceanica* (B). Bars represent the mean ± 1SE of triplicate cultures.

LITERATURE LIST

Anderson, M.A.; Morel, F.M.M.; Guillard, R.R.L., 1978. Growth limitation of a coastal diatom by low zinc ion activity. Nature 276: 70-71.

Badger M., 2003. The role of carbonic anhydrases in photosynthetic CO_2 concentrating mechanisms. Photosynthesis Research 77: 83-94.

Badger M.R.; Price, G.D., 1994. The role of carbonic-anhydrase in photosynthesis. Annual Review of Plant Physiology and Plant Molecular Biology 45: 369-392.

Barwell-Clarke J., Whitney F., 1996. Institude of Ocean Sciences nutrient methods and analysis. Canadian Technical Report of Hydrography and Ocean Sciences 182, 43p.

Brand, L.E., Sunda, W.G., and Guillard, R.R.L., 1983. Limitation of marine phytoplankton reproductive rates by zinc, manganese and iron. Limnology and Oceanography 28: 1182-1198.

Bruland K.W., 1989. Complexation of zinc by natural organic ligands in the central North Pacific. Limnology and Oceanography 34: 269-285.

Bruland K.W., Franks R.P., Knauer G.A. and Martin J.H., 1979. Sampling and analytical methods for the determination of copper, cadmium, zinc, and nickel at the nanogram per liter level in sea water. Analytica Chimica Acta 105: 233-245.

Brzezinski M.A. and Nelson D.M., 1986. A solvent extraction method for the colorimetric determination of nanomolar concentrations of silicic water in seawater. Marine Chemistry 19: 139-151.

Brzezinski, M.A., 1985. The Si:C:N ratio of marine diatoms: interspecific variability and the effect of some environmental variables. Journal of Phycology 21: 347-357.

Burkhardt S., Amoroso G., Riebesell U. and Sultemeyer D., 2001. CO_2 and HCO_3^- uptake in marine diatoms acclimated to different CO_2 concentrations. Limnology and Oceanography 46: 1378-1391.

Byrne R.H., Kump L.R. and Cantrell K.J., 1988. The influence of temperature and pH on trace metal speciation in seawater. Marine Chemistry 25: 163-181.

Claquin P., Martin-Jézéquel V., Kromkamp J.C., Veldhuis M.J.W. and Kraay G.W., 2002. Uncoupling of silicon compared with carbon and nitrogen metabolisms and the role of the cell cycle in continuous cultures of *Thalassiosira pseudonana* (bacillariophyceae) under light, nitrogen, and phosphorus control. Journal of Phycology 38 (5): 922–930.

Coale K.H., Wang X., Tanner S.J. and Johnson K.S., 2003. Phytoplankton growth and biological response to iron and zinc addition in the Ross Sea and Antarctic Circumpolar Current along 170°W. Deep Sea Research Part II: Topical Studies in Oceanography 50: 635-653.

Coale K. H., 1991. Effects of iron, manganese, copper, and zinc enrichments on productivity and biomass in the Subarctic Pacific. Limnology and Oceanography 36: 8, 1851-1864.

Crawford D.W., Lipsen M.S., Purdie D.A., Lohan M.C., Statham P.J., Whitney F.A., Putland J.N., Johnson W.K., Sutherland N., Peterson T.D., Harrison P.J. and Wong C.S., 2003. Influence of zinc and iron enrichments on phytoplankton growth in the norteastern subarctic Pacific. Limnology and Oceanography 48(4): 1583-1600.

Da Silva J.R.F. and Williams R.J.P., 1991. The biological chemistry of the elements: the inorganic chemistry of Life. Clarendon Press. Oxford, U.K.

Davis C.O., Harrison P.J. and Dugdale R.G., 1973. Continuous culture of marine diatoms under silicate limitation. I. Synchronized life cycle of *Skeletonema costatum*. Journal of Phycology 9: 175-180.

De La Rocha C.L., Hutchins D.A., Brzezinski M.A. and Zhang Y., 2000. Effects of iron and zinc deficiency on the elemental composition and silica production by diatoms. Marine Ecology Progress Series 195: 71-79.

Ellwood M.J. and Hunter K.A., 2000. The incorporation of zinc and iron into frustule of the marine diatom *Thalassiosira pseudonana*. Limnology and Oceanography 45: 1517-1524

Ellwood M.J. and Van den Berg C.M.G., 2000. Zinc speciation in the Northeastern Atlantic Ocean. Marine Chemistry 68: 295-306.

Eppley R.W. and Sloan P.R., 1966. Growth rates of marine phytoplankton: correlation with light absorption by cell chlorophyll *a*. Physiologia Plantarum 19: 47-59.

Falkowski P.G., Barber R.T. and Smetacek V., 1998. Biogeochemical Controls and Feedbacks on Ocean Primary Production. Science 281: 200-206.

Finkel Z.V., Quigg A., Raven J.A., Reinfelder J.R., Schofield O.E. and Falkowski P.G., 2006. Irradiance and the elemental stoichiometry of marine phytoplankton. Limnology and Oceanography 51: 2690-2701.

Finkel, Z.V., 2001. Light absorption and size scaling of light-limited metabolism in marine diatoms. Limnology and Oceanography 46: 86–94.

Franck V.M., Bruland K.W., Hutchins D.A. and Brzezinski M.A., 2003. Iron and zinc effects on silicic acid and nitrate uptake kinetics in three high-nutrient, low-chlorophyll (HNLC) regions. Marine Ecology Progress Series 252: 15-33.

Geider R.J. and La Roche J., 2002. Redfield revisited: variability of C:N:P in marine microalgae and its biochemical basis. European Journal of Phycology 37: 1-17.

Hales B., Karp-Boss L., Perlin A. and Wheeler P.A., 2006. Oxygen production and carbon sequestration in an upwelling coastal margin. Global Biogeochemical Cycles 20: CB 3001.

Harrison P.J., Conway H.L. and Dugdale R.C., 1977. Marine diatoms grown in chemostats under silicate or ammonium limitation. I. Cellular chemical composition and steady-state growth kinetics of *Skeletonema costatum*. Marine Biology 35: 177-186.

Ho T.Y., Quigg A., Finkel Z.V., Milligan A.J., Wyman K., Falkowski P.G., Morel F.M.M., 2003. The elemental composition of some marine phytoplankton. Journal of Phycology 39: 1145-1159.

Hutchins D.A. and Bruland K.W., 1998. Iron-limited diatom growth and Si:N uptake ratios in a coastal upwelling regime. Nature 393: 561-564.

Keller M.D., Bellows W.K., and Guillard R.L., 1988. Microwave treatment for sterilization of phytoplankton culture media. Journal of Experimental Marine Biology and Ecology 117: 279-283.

Klausmeier C.A., Litchman E., Daufresne T. and Levin S.A., 2004 Optimal nitrogen-to-phosphorus stoichiometry of phytoplankton. Nature 429:171-4.

Kovarova K., Zehnder A.J. and Egli T., 1996. Temperature-dependent growth kinetics of Escherichia coli ML 30 in glucose-limited continuous culture. Journal of Bacteriology 178: 4530–4539.

Kozelka P.B. and Bruland K.W., 1998. Chemical speciation of dissolved Cu, Zn, Cd, Pb in Narragansett Bay, Rhode Island. Marine Chemistry 60: 267-282.

Lane, T.W. and Morel F.M.M., 2000. Regulation of carbonic anhydrase expression by zinc, cobalt, and carbon dioxide in the marine diatom *Thalassiosira weissflogii*. Plant Physiology 123: 345-352.

Leblanc K., Hare C.E., Boyd P.W., Bruland K.W., Sohst B., Pickmere S., Lohan M.C., Buck K., Ellwood M. and Hutchins D.A., 2005. Fe and Zn effects on the Si cycle and diatom community structure in two contrasting high and low-silicate HNLC areas. Deep-Sea Research I 52: 1842-1864.

Lee J.G. and Morel F.M.M., 1995. Replacement of zinc by cadmium in marine phytoplankton. Marine Ecology Progress Series 127: 305-309.

Leynaert A., Bucciarelli E., Claquin P., Dugdale R.C., Martin-Jezequel V., Podaven P. and Ragueneau O., 2004. Effect of iron deficiency on diatom cell size and silicic acid uptake kinetics. Limnology and Oceanography 49: 1134-1143.

Lohan M.C., Statham P.J. and Crawford D.W., 2002. Total dissolved zinc in the upper water column of the subarctic North East Pacific. Deep-Sea Research II 49: 5793-5808.

Lynn S. G., Kilham S. S., Kreeger D. A. and Interlandi S. J., 2000. Effect of nutrient availability on the biochemical and elemental stoichiometry in the freshwater diatom Stephanodiscus minutulus (Bacillariophyceae). Journal of Phycology 36: 510–522.

MacIntyre H.L. and Cullen J.J., 2005. Using cultures to investigate the physiological ecology of microalgae. In Algal Culturing Techniques, Andersen R.A. (Ed.). Elsevier Academic Press, pp 287-326.

Maldonado M.T. and Price N.M., 1996. Influence of N substrate on Fe requirements of marine centric diatoms. Marine Ecology Progress Series 141: 161-172.

Marchetti A. and Harrison P.J., 2007. Coupled changes in the cell morphology and the elemental (C, N, and Si) composition of the pennate diatom *Pseudo-nitzschia* due to iron deficiency. Limnology and Oceanography 52: 2270-2284.

Martin-Jezequel V., Hildebrand M. and Brzezinski M., 2000. Silicon metabolism in diatoms: implications for growth. Journal of Phycology 36, 821-840.

Milligan, A. J. and Morel, F. M. M., 2002. A proton buffering role for silica in diatoms. Science 297: 1848-1850.

Morel F.M.M., Cox E.H., Kraepiel A.M.L., Lane T.W., Milligan A.J., Schaperdoth I., Reinfelder J.R. and Tortell P.D., 2002. Acquisition of inorganic carbon by marine diatom *Thalassiosira weissflogii*. Functional Plant Biology 29: 301-308.

Morel F.M.M., Reinfelder J.R., Roberts S.B., Chamberlain C.P., Lee J.G. and Yee D., 1994. Zinc and carbon co-limitation of marine phytoplankton. Nature 369:740-742.

Morel F.M.M., Hudson, R.J.M. and Price N.M., 1991. Limitation of productivity by trace metals in the sea. Limnology and Oceanography 36: 1742-1755.

Muggli D.L. and Harrison P.J., 1997. Effects of iron on two oceanic phytoplankters grown in natural NE subarctic Pacific seawater with no artificial chelators present. Journal of Experimental Marine Biology and Ecology 212 :225-237.

Muller-Karger F.E., Varela R., Thunell R., Luerssen R., Hu C. and Walsh J.J., 2005. The importance of continental margins in the global carbon cycle. Geophysical Research Letters 32: L01602.

Nelson D.M., Treguer P., Brzezinski M.A., Leynaert A. and Quequiner B., 1995. Production and dissolution of biogenic silica: Revised global estimates, comparison with regional data. Global Biogeochemical cycle 9(3): 359-372.

Pahlow M., Riebesell U. and Wolf-Gladrow D.A., 1997. Impact of cell shape and chain formation on nutrient acquisition by marine diatoms. Limnology and Oceanography 42: 1660-1672.

Parson T.R., Maita Y. and Laili C.M., 1984. A manual of chemical and biological methods for seawater analysis. Pergamon Press. New York.

Price N.M., 2005. The elemental stoichiometry and composition of an iron-limited diatom. Limnology and Oceanography 50: 1149-1158.

Price N.M. and Morel F.M., 1990. Cadmium and cobalt substitution for zinc in a marine diatom. Nature 344: 658-660.

Price N.M., Harrison G.I., Hering J.G., Hudson R.J., Nirel P.M.V., Palenic B. and Morel F.M.M., 1988/1989. Preparation and Chemistry of the Artificial Algal Culture Medium Aquil. Biological Oceanography 6: 443-461.

Pujo-Pay M. and Raimbault P., 1994. Improvement of the wet-oxidation procedure for simultaneous determination of particulate organic nitrogen and phosphorus collected on filters. Marine Ecology Progress Series 105: 203-207.

Redfield A., 1958. The biological control of chemical factors in the environment. American Scientist 46: 205-221.

Robert K., Granum E., Leegood R.C. and Raven J.A., 2007. Carbon acquisition by diatoms. Photosynthesis Research 93:79-88.

Rueter J.G. and Morel F.M., 1981. The interaction between zinc deficiency and copper toxicity as it affects the silicic acid uptake mechanisms in *Thalassiosira pseudonana*. Limnology and Oceanography 26(10): 67-73.

Sarmiento J.L. and Gruber N., 2006. Ocean Biogeochemical Dynamics. Princeton University Press. Princeton.

Shaked Y., Xu Y., Leblanc K. and Morel F.M.M., 2006. Zinc availability and alkaline phosphatase activity in *Emiliania huxleyi*: Implications for Zn–P co-limitation in the ocean. Limnology and Oceanography 51: 299–309.

Sherbakova T.A., Masyukova Y. A., Safonova T.A., Petrova D.P., Vereshagin A.L., Minaeva T.V., Adelshin R.V., Triboy T.I., Stonik I.V., Aizdaitcher N.A., Kozlov M.V., Likhoshway Y.V. and Grachev M.A., 2005. Conserved Motif CMLD in silicic acid transport proteins of diatoms. Molecular Biology 39: 269-280.

Skrabal S.A., Lieseke K.K. and Kieber R.J., 2006. Dissolved zinc and zinc-complexing ligands in an organic-rich estuary: Benthic fluxes and comparison with copper speciation. Marine Chemistry 100: 108-123.

Strzepek R.F. and Harrison P.J., 2004. Photosynthetic architecture differs in coastal and oceanic diatoms. Nature 431: 689-692 .

Sun J. and Liu D., 2003. Geometric models for calculating cell biovolume and surface area for phytoplankton. Journal of Plankton Research 25: 1331-1346.

Sunda W.G. and Huntsman S.A., 2005. Effect of CO_2 supply and demand on zinc uptake and growth limitation in a coastal diatom. Limnology and Oceanography 50(4): 1181-1192.

Sunda W.G., Price N.M. and Morel F.M.M., 2005. Trace metal ion buffers and their use in culture studies. In Andersen R.A. [Ed.] Algal Culturing Techniques. Elsevier Academic Press, pp 35-63.

Sunda W.G. and Huntsman S.A., 1995. Cobalt and zinc interreplacement in marine phytoplankton: Biological and geochemical implications. Limnology and Oceanography 40(8): 1404-1417.

Sunda W.G. and Huntsman S.A., 1992. Feedback interactions between zinc and phytoplankton in seawater. Limnology and Oceanography 37(1) 25-40.

Takeda S., 1998. Influence of iron availability on nutrient consumption ratio of diatoms in oceanic waters. Nature 393: 774-777.

Thamatrakoln K. and Hildebrand M., 2008. Silicon uptake in diatoms revisited: a model for saturable and nonsaturable uptake kinetics and the role of silicon transporters. Plant Physiology 146: 1397-1407.

Treguer P., Nelson D.A., van Bennekom A.J., DeMaster D.J., Leynaert A. and Queguiner B., 1995. The silica balance in the world ocean: a re-estimate. Science 268, 375-379.

Van den Berg C.M.G., Merks, A.G.A. and Duursma, E.K. (1987). Organic complexation and its control of the dissolved concentrations of copper and zinc in the Scheldt estuary. Estuarine, coastal and Shelf Science 24: 785-797.

Westall J.W., Zachary J.L., and Morel, F.M.M., 1976. MINEQL. Technical Note #18. R.M. Parsons Laboratory for Water Resources and Hydrodynamics, Department of Civil Engineering, Massachusetts Institute of Technology, Cambridge, Massachusetts.